Microbial fuel cell-based biosensor for redox potential detection in fermentation process

A Thesis Submitted to the
College of Graduate and Postdoctoral Studies
In Partial Fulfillment of the Requirements
For the Degree of

Master of Science

In the Department of Chemical and Biological Engineering
University of Saskatchewan
Saskatoon

By

Siyang Shen

PERMISSION TO USE

In presenting this thesis in partial fulfilment of the requirements for a Master of Science degree from the University of Saskatchewan, I agree that the Libraries of this University may make it freely available for inspection. I further agree that permission for copying of this thesis in any manner, in whole or in part, for scholarly purposes may be granted by the professor or professors who supervised my thesis work or, in their absence, by the Head of the Department or the Dean of the College in which my thesis work was done. It is understood that any copying or publication or use of this thesis or parts thereof for financial gain shall not be allowed without my written permission. It is also understood that due recognition shall be given to me and to the University of Saskatchewan in any scholarly use which may be made of any material in my thesis.

Requests for permission to copy or to make other uses of materials in this thesis/dissertation inwhole or part should be addressed to:

Head of the Department of Chemical and Biological Engineering
University of Saskatchewan
57 Campus Drive
Saskatoon, SK, S7N 5A9, Canada
OR
Dean
College of Graduate and Postdoctoral Studies
University of Saskatchewan
116 Thorvaldson Building, 110 Science Place
Saskatoon, SK, S7N 5C9, Canada

ABSTRACT

Currently, fermentation research's primary objective is to develop economic and sustainable processes by increasing the product yield and reducing the operating cost. A tremendous effort had been made in the past few decades by discovering and developing various fermentative strains. The fermentation process measurement, control, and supervision are the next battlefield for further fermentation technology development. Fermentation manipulation is a complex process from both biological and engineering points of view. Different factors, including substrates type, substrates concentration, strain type, and operating modes, need to be taken into account. These aspects encourage the scientific community to find a robust, sophisticated, and versatile measure for controlling fermentation.

Redox potential, also known as the oxidation-reduction potential (ORP), reflects the overall biochemical reactions, electron transfer, and redox balance within the fermentation broth. The biological significance of ORP includes indirectly explicating metabolic activities during fermentation and regulating the metabolic network, affecting the metabolic pathway and gene expression. The monitoring and controlling environmental ORP provides a thoughtful understanding to help control the intracellular metabolic activities and fermentation process. This approach has been proven and considered as a real-time approach to increase fermentation efficiency in scientific communities and industrial sectors. In particular, the ORP measurement can provide an online and consistent signal during fermentation. It can be used at any stage of fermentation, providing both high signal-integrity and measurement reliability. Although effective, the relatively high fabrication cost of these sensors has so far made it impractical for extensive applications in large-scale contaminated soil monitoring, in particular.

Cost-effectiveness is an endless effort in engineering, an economically optimized ORP monitor tool is urgently needed. With the development of bio-electrochemical research, the microbial fuel cell (MFC) as an old technology has been adopted as a biosensor to produce power and electricity by bacteria catalyzation. In this work, an MFC-based biosensor device was designed and developed as a fermentation biosensor using an indigenous microorganism and modified Nernst equation to integrate among the MFC voltage output, fermentation ORP, and fermentation stages.

This study investigated different factors on the performance of an MFC-based biosensor. These factors include strain types (*Bacillus subtilis* and *Pseudomonas fluorescens*) in the presence or absence of methylene blue mediator, cathodic treatments (sparging, aerated cathode, and potassium ferricyanide solution), and anodic aeration rates (0, 11.32, and 22.64 vvm). After optimal conditions were established, this study used turbidimetric measurement as the indicator for microbial growth. The correlational between microbial growth and ORP, voltage, potential parameter (X) were investigated. Results showed that *B. subtilis* exhibited superior performance under MFC condition. Sparging cathodic treatment provided a feasible and sustainable supply of electron acceptor. Keeping anodic aeration rate at 11.32 vvm constructed a suitable anodic environment not only to support *B. subtilis* growth but also to sustain the voltage generation from MFC device. After all conditions had been settled, the voltage signal was projected to a linear increase, and the ORP signal was likely to generate a bathtub-shaped curve. Two peaks occurred on the curve by integrating both signals into the potential parameter X and plotting the potential parameter X over time. Three distinct growth phases were revealed by comparing the potential parameter X with microbial growth information and ORP profile. Potential parameter X indicated the endpoint of lag phase, mid-point of exponential phase, and the starting point of stationary phase. Such a result proved that the potential parameters could provide fruitful and high-resolution information that enables precious and real-time fermentation monitoring and controlling. To conclude, this thesis demonstrated the development of a novel fermentation biosensor by utilizing an MFC device as a biosensor. By applying the unitless parameter (i.e., potential parameter) derived from the modified Nernst equation, an MFC device equipped with an ORP sensor could successfully unveil the hidden internal information during the course of fermentation and explicate microbial growth dynamics.

Although successful, many questions were also raised during the course of this research. One main limiting factor the choice of the microorganism. In this research, *Bacillus subtilis* was selected as it could generate extracellular electrons which then pick up by the carbon electrode in anodic chamber, resulting in voltage flow. When different microbes were chosen, one needs to investigate whether such a microbial strain could export electron in MFC device. If not, one could attempt to supplement electron mediator to assist electron movement from microbial surface to carbon electron. The operating condition for this developed device needs to be optimized as different strains possess different growth requirements.

ACKNOWLEDGEMENTS

I want to express my deepest gratitude to my supervisor, Dr. Yen-Han Lin, for his insightful advice, patience, and invaluable support. I feel very fortunate to have him as my advisor and to have the opportunity to work with him for the past two years. He has always been available and willing to provide unerring advice. Working with him made this journey very pleasantly, and for that, I am deeply grateful.

Thanks to my committee: Professor Hui Wang and Professor Catherine Niu, whose suggestions have also shaped this thesis, their supervision allowed develop and elaborate new ideas. I am deeply grateful to all the faculty and staff in the department, especially Kevin Carter, Majak Mapiour, RLee Prokoishyn, and Dushmanthi Jayasinghe, for their help during my research.

I would also like to recognize my friend and colleague Xiaoyan Huang spent countless hours educating me with myriad skills and knowledge and providing unfailing advice and encouragement during my research.

I also feel it is important to mention my gratitude to my girlfriend Yingxin Wang, who has offered unconditional support and provided care in my daily life. Thank you for the endless love, encouragement, support, and patience.

Last but not least, my love and gratitude to my parents, Wangtao Ruan and Jiqin Shen, for raising me to always strive for success, providing endless love and financial support. At the same time, I work toward my bachelor's and master’s degrees.

TABLE OF CONTENTS

LIST OF FIGURES

NOMENCLATURE

List of Abbreviation

ATP Adenosine triphosphate

BOD Biological oxygen demand

COD Chemical oxygen demand

DO dissolved oxygen

GHG Greenhouse gases

GSSG/GSH Glutathione

LB Lysogeny broth

MFC Microbial fuel cell

NAD^+/NADH Nicotinamide Adenine Dinucleotide

$NADP^+$/NADPH Nicotinamide adenine dinucleotide phosphate

OD Optical density

ORP oxidation-reduction potential

OX oxidant

PEM Proton exchange membrane

PVA Polyvinyl alcohol

RED reductant

Roman Symbols

Symbol	Description	Unit
A	Surface area	cm^2
a	Gap width	μm
CY_{nor}	Coulombic yield under normal condition	%
CY_{tox}	Coulombic yield under toxic condition	%
c	Analyte concentration	mM
E_{cell}	Actual cell potential	mV
E_{anode}	Anode potential	mV
$E_{cathode}$	Cathode potential	mV

F	Faraday constant	C/mol
I	Current	mA
G	Bacterial biofilm conductance	μS
g	Thickness of biofilm	μm
K	Reaction equilibrium constant	Mole L^{-1}
K_s	Half-velocity constant	g/mL
L	Length of electrode	cm
n	Number of transferred electrons	-
Q_r	Reaction quotient	-
R	Ideal gas constant	$J \cdot K^{-1} \cdot mol^{-1}$
T	Temperature	Kelvin
V	Voltage	mV
vvm	Aeration rate	L L^{-1} min^{-1}
x	potential parameter	-

Greek Symbols

Symbol	**Description**	**Unit**
η_{act}	Activation polarization	mV
η_{con}	Concentration polarization	mV
η_{ohm}	Ohmic loss	mV
μ	Bacterial growth rate	min^{-1}
σ	Electricity conductivity	μS/cm

1 INTRODUCTION

The fermentation technology predates science. Harnessed for food production and preservation, it appears in varied cultures from all over the world, throughout recorded history. Before the era of modern storage, storage technologies were limited, and spoiling was a significant issue for humanity, fermentation enables the production of long-term storable food. It has been a crucial part of human culinary history and plays a vital role in the development of civilization (Zilberman & Kim, 2011). Biochemically, fermentation is the most common activity that is widely distributed in all biological systems. Microorganisms such as bacteria and eukaryotes perform metabolic activities by degrading organic substrates to obtain energy from ATP synthesis.

Traditionally, the typical products of fermentation as foods were limited. Since the establishment of modern microbiology by Pasteur in the 19th century, the domestication of microorganisms became possible. Fermentation has emerged and flourished as an industry, producing and modifying such foods as cheeses, yogurts, vegetables, fruits, meat, and alcohol. Until today, modern industrial fermentation has become a pillar of modern industry and extended its definition to convert raw materials into industrial products (Humphrey & Lee, 1992). The rapid development of biotechnology accelerates the growth of fermentation industry from diverse sectors over the last several decades, the major products of fermentation include but are not limited to food, beverage, amino acids, biopolymers, biofuel, solvents, and drugs (Coton et al., 2017). Economically, the size of global fermentation chemical market values around 58.68 billion U.S. dollar in 2018 (GrandViewResearch, 2019), with alcohols, enzymes and organic acids comprising its largest sectors.

Furthermore, fermentation is considered environmentally friendly as it utilizes sustainable resources and emits relatively low greenhouse gas (GHG), thereby maintaining a small carbon footprint. Increased ecological awareness among consumers is driving growth and investment in fermentation as a key player in our increasingly bio-aware society (Asveld & Van Est, 2011).

Since 2000, studies have discovered that extremophilic microbes had special metabolic utility for industrial fermentation. New areas of research quickly emerged in the biodiesel, biogas,

and bioremediation sectors (María Martínez-Espinosa, 2020). Commercial applications aim to optimize the quality and quantity of final product in a large-scale operation through the manipulation and monitoring of the microbial biochemical processes. Nevertheless, the microorganism plays a crucial role in the fermentation process. While dissolved oxygen (DO) measurement is one of the most common assays, anaerobic or micro-aerobic cultures will not produce sufficient oxygen for this to work. Since other parameters, such as pH or temperature, are incapable of reflecting the actual cell metabolic states within the fermenter (Liu et al., 2013), the redox potential, or oxidation-reduction potential (ORP), has been proposed as a promising alternative for the online monitoring of anaerobic fermentation processes (Bonan et al., 2020).

ORP is an electrochemical measure of the reactive chemical environment within a solution that determines the rate and type of redox reaction. More importantly, the biological redox system plays an essential role in microbial metabolism. ORP reflects the overall electron movement and redox balance for both intracellular and intercellular of a biological system. Measurement of ORP of the system appears to be a valid approach to investigate the dynamics of microbial metabolism. A previous study (Liu et al., 2013) shows the enzymes related to the oxidation and reduction reaction in a biological system are redox potential sensitive, impose redox potential regulation, and redirect intracellular metabolic flux to desired secondary metabolite product, eventually leading towards more effective fermentation outcome. However, a problem arises in that an ORP sensor (constructed of an Ag/AgCl reference electrode, 99% pure platinum band encapsulated in the potassium chloride solution, and the electrode itself) is prone to fouling. Any disturbance in solution or metabolic residual on the sensor surface will lead to misrepresentative readings. Furthermore, the high fabrication cost and maintenance costs of such a sensor limit the ORP technique to the large scale of industrial fermentation.

A microbial fuel cell (MFC) is a device that generates electricity from anaerobic microbes. In a typical MFC, the microorganisms in the anodic chamber oxidize the substrate, producing protons and electrons. The latter then travel through an external circuit to the cathodic chamber, generating a voltage between the two chambers. Accordingly, intracellular electron transfer and redox balance, driven by the metabolism of microorganisms, affects the ORP. The MFC then detects and captures the electrons within the extracellular environment and generates an electrical signal. Intriguingly, the MFC has the dual benefit of serving as both a power generator and a cost-effective replacement for the fermentation redox sensor. Although MFCs remain novel as

biosensors, ongoing research includes environmental carbon and toxin detection (Chouler & Di Lorenzo, 2015; Cui et al., 2019; Do et al., 2020; Zhou et al., 2018) as well as use as an ORP sensor.

The overall goals of this research are to investigate and elucidate the relationship between electricity generation and ORP variation within an MFC system and determine the suitability of integrating an MFC device with an ORP sensor. In this thesis, Chapter 1 outlined the fermentation and industrial fermentation from a historical perspective and briefly introduced the ORP technology and MFC technology. Chapter 2 provided a review on the importance of ORP at the biological level, the utilization of ORP technology for fermentation, and the application of current MFC technology for both electricity production and biosensing. Chapter 3 listed the choice of microorganisms, the materials used in an MFC device, data collection procedure, and analytical methods used in this thesis. Chapter 4 illustrated the derivation of the Nernst equation, different microbial strains, different cathodic and anodic treatments on MFC-based biosensor performance, and the correlation among microbial growth, ORP, MFC, and potential parameter under MFC conditions. Chapter 5 concluded this thesis by reformulating the Nernst equation, and a tight relationship that associated between ORP and voltage production in an MFC device. Finally, some possible future applications and improvements of the developed MFC-based biosensor were also provided in Chapter 5.

2 LITEATURE REVIEW

2.1 Background

2.1.1 Introduction to redox potnetial

Redox potential (ORP) is a specific indicator of its oxidizing or reducing power intensity depending on the electrochemical balance. The redox potential is the outcome of the redox (oxidation and reduction) reaction within the system. While the redox reaction is one of the most fundamental biochemical reactions, the modern exploration of redox research only traces back to the 18th century. After the scientific community overthrew the old phlogiston theory, Antoine-Laurent Lavoisier proposed a widely-accepted explanation of combustion, which elucidated the nature of oxygen, identified oxygen as an essential element for discharge, and recognized the oxygen and hydrogen elements soon after (Karamanou & Androutsos, 2013). The theory is widespread and accepted by the research community. Scientists concluded that reactions in which oxygen was consumed were classified as oxidation, while those in which oxygen was lost were term reductions. The rapid development of electrochemistry during the 19^{th} and 20^{th} centuries shed further light on the redox reactions, which were soon implicated in the galvanic cell: ferrous ions could change ferrous oxide at the anodic electrode, though the full underlying principles were not yet clear (Ferguson, 1923).

In 1956, Rudolph A. Marcus developed the first electron transfer theory which elucidated the driving force of redox reaction and interpreted the redox reaction's rate by a parabola (Marcus, 1956). His theory explains oxidation and reduction reactions, laying a foundation for further electrochemical and biological research, and he was awarded the Nobel prize in chemistry in 1992. Integrating Marcus's theory with the electronegativity scale, Jensen set standards of redox potential, which could be used to monitor the redox dynamics of a system (Jensen, 1996).

A redox reaction involved two components, including oxidizing agent which gain electron to form a reducing agent, as described by:

$$Ox + ne^{-} = Red \tag{2.1}$$

In a redox reaction, the electron is transferred between the redox pair. Both oxidation and reduction reactions take place simultaneously. For example, consider the reduction of copper by zinc, which can be viewed as two half-reactions:

Oxidation reaction: $Zn \rightarrow Zn^{2+} + 2e^{-}$ (2.2)

Reudction reaction: $Cu^{2+} + 2e^{-} \rightarrow Cu$ (2.3)

Overall reaction: $Zn + Cu^{2+} \rightarrow Cu + Zn^{2+}$ (2.4)

For the reduction half reaction, the equilibrium constant for the reaction can be represented as:

$$K = [Cu]/[Cu^{2+}][e^{-}]^2 \quad (2.5)$$

Rearranging the above equation, we see that the electron activity of redox potential can be isolated as:

$$e^{-} = [\,[Cu]/(K * [Cu^{2+}])]^{\frac{1}{2}} \quad (2.6)$$

or

$$pE = -\log e^{-} = \frac{1}{2}[\log K - \log \frac{(Cu)}{(Cu^{2+})}] \quad (2.7)$$

The standard redox potential between two different chemical species can be predicted by redox half-reaction. By determining the potential difference between the chemical reaction and a standard hydrogen electrode, a standard redox potential table of any chemicals and chemical species can be established. The standard redox potential is a systematic measurement that represents the intrinsic capacity of molecules or chemical half reactions' tendency to be either reduced or oxidized. Similarly, using this relationship, a standard redox potential table can be produced to give the intrinsic capacity of molecules or chemical half-reactions to be reduced or oxidized. A lower redox potential indicates a reductive state prone to losing electrons and vice versa. The difference in redox potential between an electron donor and an acceptor determines the driving force of the electron transfer reaction:

$$\Delta \mathrm{G} = -n * F * \Delta \mathrm{E} \quad (2.8)$$

where n is the number of electrons transferred, F is the Faraday constant, and ΔE is the difference in redox potential. Generally, the standard redox potential for a half-reaction in an aqueous solution is based on the assumption that the concentration of all chemical species is 1 molarity. In practice, the reaction kinetics are complex and depend on the specific molarities. Typically, the Nernst equation is used to define the redox potential in an aqueous system (Chang et al., 2004):

$$E_{cell} = E^{\emptyset}_{cell} - \frac{RT}{n\mathrm{F}} \ln Q_r \quad (2.9)$$

On the other hand, the actual measurement of the redox potential typically uses an ORP sensor, which is constructed with a chemically inert electrode (such as platinum, nickel, and gold) immersed in the solution as a reference. A reference electrode made with silver-silver chloride (a structure similar to a pH sensor) is connected to saline solution and poses a neutral half cell potential. A simplified diagram and ORP sensor are present in Figure 2.1.

The redox potential is measured in volt (V) or millivolt (mV), the inert electrode sensing the dissolving electrode ion and returning electrode ion to define the potential and compare the difference between a solution with a stable reference electrode to generate redox reading. Because platinum is highly conductive yet has low chemical and biological reactivities, it is an ideal material for the redox probe. However, any impurity or (in)organic buildup on the probe will lead to a false reading. Thus, frequent maintenance, recalibration, and replacement of redox sensor are required for long-term measurement stability when the redox monitoring project goes online (Suslow, 2004).

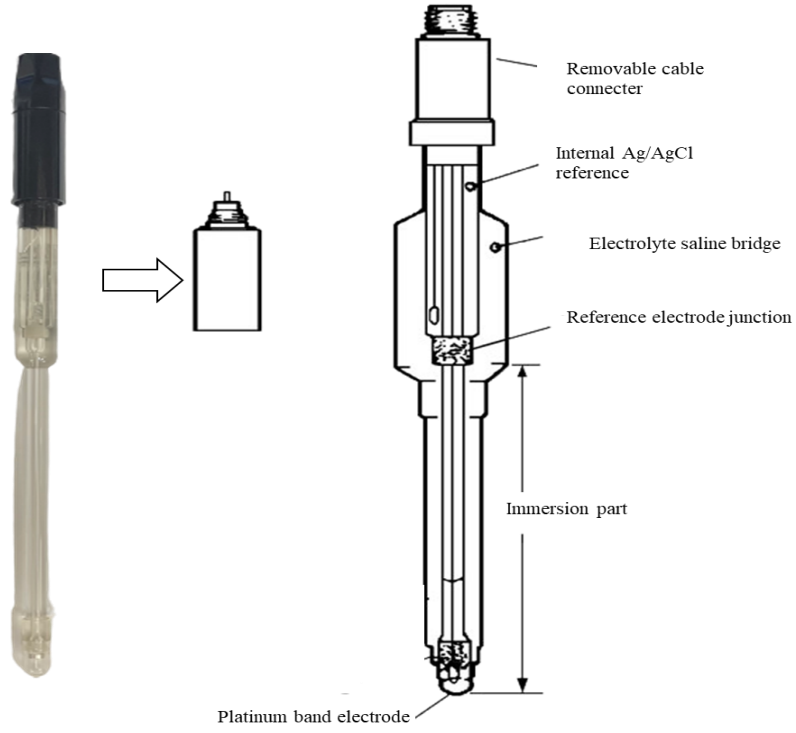

Figure 2.1 Diagram of a laboratorial ORP sensor.

2.1.2 Fermentation redox potnetial

Redox reaction is a fundamental type of chemical reaction in biological systems (from cells to flora and fauna). Living organisms obtain energy for maintenance, growth, reproduction motility,

and other functions from the redox reaction (Shapiro, 1972). Redox reaction involves both energy metabolism and the biological redox process, which take place simultaneously. The significance of redox potential for cellular metabolism study was predicted by Joseph Needham in 1926, and great research interests have been drawn to the scientific community since then (Cohen et al., 1928; Needham & Needham, 1926).

The shift of redox potential relates to the electron movement in the biological system, and the role of electron transfer has been investigated and established (Lande et al., 2012). However, those studies only focused on the underlying biochemical mechanism of electron transfer, and a standard protocol to observe the electron transfer under experimental conditions is still under investigated. There are several difficulties in measuring electron transfer in the biological systems, which include: (1) reactions are mostly not self-exchange; (2) structural information is often obscured; (3) environments are often inhomogeneous; (4) standard free energy remains undefined; (5) reactions might occur across membranes; and (6) reations might involve protein conformation; (7) a fixed reaction site is absent (Marcus & Sutin, 1985).

On the biochemical level, energy storage/release is one of the essential examples of redox electron transfer. Adenosine triphosphate (ATP) synthesis relies on the degradation of organic matter via oxidative phosphorylation. The pathways of ATP synthesis impact a full range of biomolecules, including carbohydrates, amino aicds, fatty acids, and nucleic acids. A balance must be maintained between oxidizing and reducing agents; otherwise adversely biological effects will arise (Foyer & Noctor, 2005). For example, an unbalanced redox state leads to reactive oxygen, sulfur, and nitrogen species, which can impair protein translation, modification, and cellular signaling (Jones & Sies, 2015). Redox homeostasis is fundamental for maintaining regular cellular function, and redox potential offer an essential window for perceiving and evaluating the state of a biological system. Owing to the complexity of biological redox system, there is no direct approach for sensing the intercellular redox potential. Instead, the redox state may be summarized by the presence of a redox couple within the system (Schafer & Buettner, 2001).

There are three prominent redox couples that can be used as the indicators for defining the intercellular redox potential, which are NAD^+/NADH, $NADP^+$/NADPH, and GSSG/GSH. NAD^+/NADH and $NADP^+$/NADPH are used to estimate the reduction potential, and GSSG/GSH facilitates the oxidation potential evaluation. (Wang et al., 2018). In these redox couples, NAD^+/NADH is the most abundant in the intercellular environment. In the sense of bioenergetic

metabolism, the cycle between NAD^+ and its reduced form, NADH, contributes a reducing potential to the mitochondrial electron transport, fuelling phosphorylation in ATP synthesis. The NAD^+/NADH cycle also plays roles in the nucleus and cytosol as well as extracellularly. Cantó et al. (2015) concluded that the NAD^+ and NADH equilibrium played an important role in regulating cellular flux rate and direction. The concentration of NAD^+ and NADH have typically maintained between 0.2 to 0.5 mM, but significant shifts might occur under environmental change and energy stress (Fig 2.2). This discovery showed the potential for scientists to control cellular metabolism by altering the intercellular and intracellular redox environments.

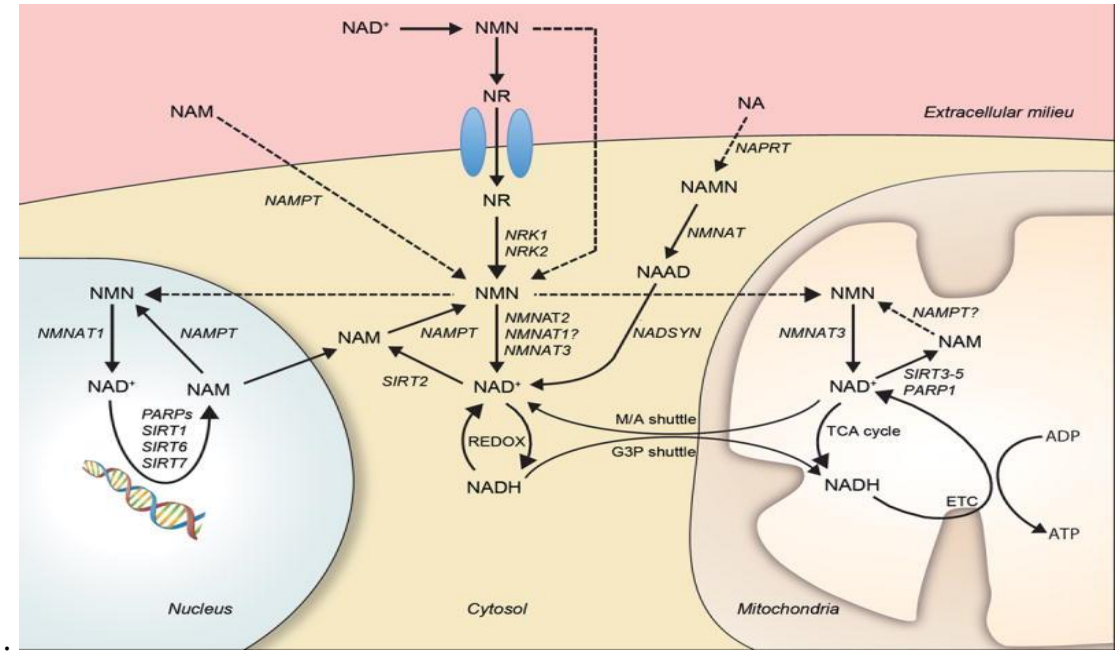

Figure 2.2 NAD^+/NADH cross compartment metabolism (Cantó et al., 2015)

2.1.3 Curreent redox potential application in fermentation

Traditionally, fermentation refers to cellular respiration without oxygen as the terminal electron acceptor. However, with the improvement of biotechnology, the definition of fermentation has been broadened to include the production of biomolecules such as amino acids, proteins and polysaccharides, and substance such as ethanol and organic acids, by microorganisms under both aerobic and anaerobic environments (María Martínez-Espinosa, 2020). Specifically, fermentation is a microorganic extraction of energy via the glycolysis pathway, where pyruvate is produced, followed by reduction to the secondary metabolites. Figure 2.3 shows the electron movement within the redox pair of NADH and NAD^+. This conversion directly alters the

intercellular redox potential, affecting the abundances of some important biomolecules such as ATP, amino acids, fatty acids, and nucleic acids. Since redox potential represents the sum of total redox reactions undergoing metabolism within the cells, the redox potential is also strongly affected by environmental factors such as pH, dissolved oxygen levels, and response equilibria (Ishizaki et al., 1974). Further effects include the exchange of free oxygen and hydrogen through (semi)permeable membranes due to shuttle-protein activity. Thus, redox potential is manipulable externally and also provides an alternative approach to understanding and monitoring the fermentation status.

Elaboration is first on monitoring and then on manipulating: (1) The solution redox potential measures the concentration of nutrients and reducing agents as well as the medium's oxygen level. Typically, in batch fermentation, the redox potential profile follows a bathtub-shaped curve (Liu et al., 2017). As presented in Figure 2.4 (Liu et al., 2017), the microbial population size remains small during “the lag phase”, but the medium maintains high oxygen and nutrient levels. The redox potential remains at its high initial point, undergoing a subtle decline. After entering “the log growth phase,” the microorganism population surges. Nutrients and oxygen deplete with the rapid increase in cell number, resulting in a dramatic decrease in solution redox potential. Eventually, due to the depletion of nutrients and a reduction of culture vitality, the older cells undergo apoptosis, releasing the organic matter back into the environment. At this point, an abrupt increase of redox potential indicates that the batch fermentation is approaching the endpoint. This feature, with its rapid response time and high sensitivity to the redox reaction, has become a key heuristic for online fermentation monitoring. (2) The internal processes can be re-directed by imposing a redox potential regulation strategy in the external environment, which include gene expressions and enzyme activities (Allen, 1993) to optimize desired secondary metabolites – thus achieving a higher input-output ratio for feedstock and reducing total operation time (Liu et al., 2017).

Sparging is the most common method to control redox potential during fermentation. For aerobic strains, by using dissolved oxygen acts as a terminate electron acceptor and by controlling the aeration rate and the air-nitrogen concentration, a target redox potential level can be achieved. With semi-aerobic or anaerobic strains, the oxygen must be replaced by a different oxidizing agent, such as potassium ferrocyanide. In both cases, the optimum redox potential level depends on many factors: specific strain, substrate, and objective metabolites. As examples:(a) Bonan et al. (2020)

reported about xylose fermentation with yeast (Spathaspora passalidarum) and found an optimum yield (28.61g/L) occurs for a redox potential reading of -100mV. (b) A study of ethanol production in high gravity found that with a highly concentrated 250g/L glucose substrate, a redox potential of -150mV led to both an optimized yield of 131g/L and assisted yeast survival under the harsh osmotic pressures. (c) In commercial wine fermentation, Killeen et al. (2018) showed that a redox potential of 215mV accelerated the fermentation process and maintained yeast cell viability compared to a control group. More importantly, the redox potential control strategy was shown to enhance exogenous gene expression during fermentation via redirecting the metabolic flux. (d) Zhu et al. (2009) utilized a two-stage redox potential control strategy to increase production of 3-hydroxy propionic acid via a recombinnant *Klesiella pneumoniae* strain.

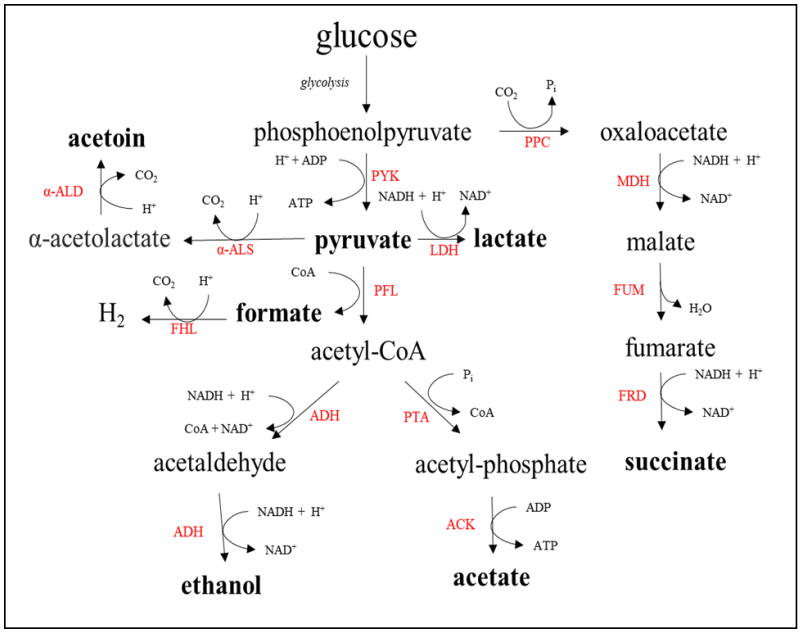

Figure 2.3 NAD^+/NADH redox couple in pyruvate fermentative degradation

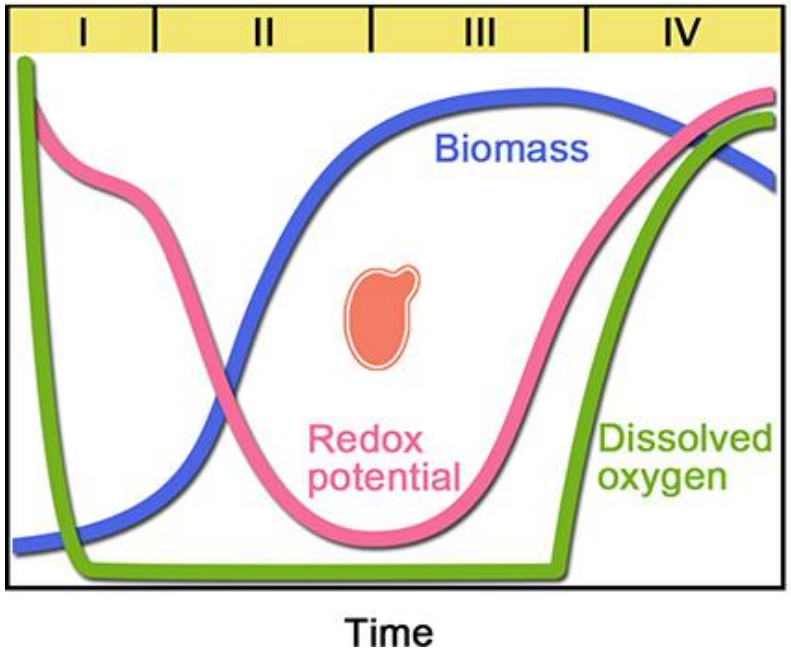

Figure 2.4 Bathtub-shaped curve of ORP profile during fermentation (Liu et al., 2017)

2.1.4 Introduction to microbial fuel cell

Due to the increasing energy demand and concern for long-term energy security, the study of the microbial fuel cell (MFC) has been flourishing in recent years. This technology integrates biophysical chemistry and electrochemistry to utilize the biocatalytic capability of the microorganism to stimulate a bioreactor that spontaneously converts organic matter to electrical energy through the metabolic activity of microbe (Logan et al., 2006).

Microorganisms, usually bacteria, continually catalyzes organic substrate into the inorganic matter and renewable electricity in the MFC. The substrate selection varies depending on the choice of bacteria or bacterial consortium and the growing environment. Furthermore, microbes could contribute to the bioremediation of industrial waste as well. Multiple studies had been reported that the MFC device could assist in the bioremediation of pollutants and the economic feasibility of utilizing microbial fuel cell (Chen et al., 2016; Li et al., 2019; Morris & Jin, 2008; Pous et al., 2013). With the dual benefits of generating renewable energy and bioremediation by degrading pollutants, microbial fuel cell seems to be a promising yet challenging technique for the future.

The following section will discuss the history of MFC technology, the principle, mechanism, configuration of different types of primary microbial fuel cells, and the applications of this technique.

2.1.4.1 Development of microbial fuel cell technology

In 1791, the Italian physician and physicist Luigi Galvani birthed the field of bioelectricity when he detected electricity in frog muscle tissue (Park et al., 2013). After a century, Potter (1912) constructed the first microbial fuel cell when he demonstrated–that electrical energy could be liberated from organic compounds by a culture of *Escherichia coli* and *Saccharomyces spp.* Inspired by Potter, Cohen (1931) connected multiple MFCs in series, producing over 35 volts of electricity.

Davis and Yarbrough (1962) utilized hydrocarbon as the carbon source for the MFC to generate electricity. Although no electrical output was observed, this is the first attempt to apply MFCs to the problems of biodegradation and bioremediation. In the same year, Rohrback et al. (1962) successfully generated hydrogen by *Clostridium butyricum* culture within a glucose oxidase electrode system.

In the 1980s, it was understood that a critical limitation of microbial fuel cells lies in electron transport efficiency. Peptidoglycans and lipopolysaccharides in the bacterial membrane greatly impeded the movement of electrons was recognized (Du et al., 2007). Several efforts were made to chemically mediate the electron transfer (Weibel & Dodge, 1975; Yaropolov et al., 1976). In 1993, a functioning mediated MFC that could transport electrons without an endogenous electron shuttle was developed (Allen & Bennetto, 1993). Those improvements yielded a significant improvement in power output and spurred widespread interest in MFCs worldwide. Unfortunately, applications were limited because the necessary mediator concentration was poisonous to the microorganism (Logan et al., 2006). The development of the mediator-less MFC sparked a revolution.

In exploring how electron transfer within an MFC occurs, researchers discovered certain species of bacteria capable of transferring electrons directly – without a mediator. Kim et al. (1999) reported the first self-electron transfer bacterium *Shewanella putrifaciens*. Chaudhuri and Lovely (2003) confirmed their finding by demonstrating that *Rhodoferax ferrireducens* can oxidize glucose to carbon dioxide by self-shuttling the electron to the electrode without the assistance of any mediator. Gorby et al. (2006) reported that a special nanowire is produced by a mutated strain

of *S. oneidensis*, which enables the direct electron transfer in bacteria. These findings led to many practical applications of the mediator-less MFC such as: long-term and remote energy-generation (deep-sea sensors, military and robotic devices) and in wastewater treatment (Singh & Yakhmi, 2014).

2.1.4.2 Type of microbial fuel cell

MFC architecture can vary by size, design, and material yet broadly fall into two classes: single- and double-chambered configurations. As illustrated in Figure 2.5, the double-chambered MFC consists of anodic and cathodic chambers divided by a proton exchange membrane (PEM), which permits proton-crossover from the anodic chamber yet blocks oxygen diffusion from the cathodic compartment. The electron provided by the anode combines with the proton as an electron acceptor at the cathode to complete an external circuit. Double-chambered MFCs often operate in a batch mode with the use of defined medium (Logan et al., 2006).

The "H-shape" is one of the most commonly double-chambered MFC configurations for research as the design can be easily modified for different objectives by altering the electrode, chamber size, material, and/or half-cell condition. Sangeetha & Muthukumar (2012) reported that closely spaced electrodes yield elevated power output and chemical oxygen demand (COD) removal when using wastewater as a substrate. By contrast, the wide electrode separation of H-configured MFCs results in a greater internal resistance, leading to poor power output (Du et al., 2007).

Miniature MFCs are another double-chambered configuration that has intrinsic advantages for research. Ringeisen et al. (2006) reported that a 1.2 cm^3 working volume of MFC is capable of producing 10 mW/m^2 of maximum power density, which is sufficient for autonomous sensors located in remote areas. Other advantages of miniature MFCs include: a short startup time, more negligible material consumption, and higher throughput of power. (Jiang et al., 2015). Such features enable MFC utilization in the technical area, such as the remote robot, submarine camera, or self-sustainable energy devices.

Up-flow MFCs evolved from an up-flow anaerobic sludge blanket reactor design into a two-chamber configuration, yielding a maximum power output of 170 mW/m^2(He et al., 2005). This device received a lot of attention because it can be easily scaled to treat large volumes of wastewater (Du et al., 2007). A modified version with a U-shape PEM, featuring a larger surface area while decreasing the electrode separation, and achieved a significant power boost of 29.2

W/m^2 as the internal resistance declined from 84 Ω to 17Ω (2006). Note that the up-flow MFC design is not viable as a bio-generator because the recirculation pumps consume more power than the device generates (Du et al., 2007).

In single-chamber MFCs, the cathode is either outside the fuel cell cavity or inside without using a PEM-(Logan et al., 2006). Eliminating PEM, which costs roughly US$1400/$m^2$ (Nafion®), removes a major obstacle for the large-scale commercialization of MFCs. Additionally, Oliveira et al. (2013) suggested that during continuous operation, the presence of a PEM can cause acidification of the anode compartment leading to degraded performance. Using wastewater as a substrate, Liu and Logan (2004) tested these ideas and achieved similar efficiencies with and without a PEM. However, with glucose as a substrate, the PEM-equipped designs were much more efficient (40-55% vs 9-12%).

Follow-on studies investigated novel and low-cost substitutes for the PEM. Li et al. (2011) classified separator technology into ion-exchange membranes, size-selective separators, and salt bridges. Chang et al. (2017) produced 38 mW /m^2 electricity using a low-cost PVA separator. Even though single-chamber MFCs typically generate lower energy output, they remain preferable for real-world applications because their simplified design is cost-effective, scalable, and lowering operational difficulty.

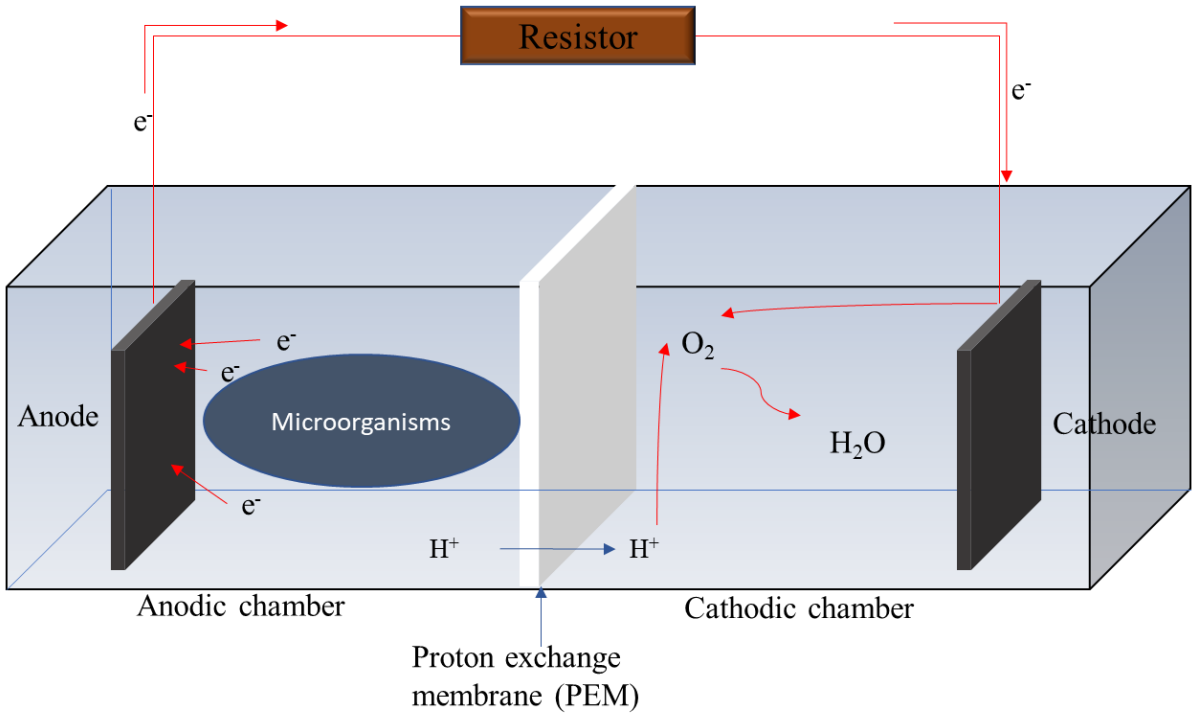

Figure 2.2.5 Schematic diagram of a double-chambered microbial fuel cell

.

2.1.5 Fundamental mechanism of MFC

The configurations of the MFC are varied significantly depending on the size, material selection, and applications. A typical MFC consists of an anodic and a cathodic chamber separated by a half-cell separator. Figure 2.5 provides a schematic view of one of the most widely used dual chamber MFC configurations. The substrate is oxidized by microorganisms anaerobically in the anodic chamber. The proton passes freely through a half-cell separator, inhibiting oxygen and ions crossover through a proton gradient.

The microbe liberates electrons from the organic substrate at the anode. The generated electrons are transferred through an external circuit, subsequently consumed by the cathodic compartment. The electrical potential is brought about by the bacterial activity in the anodic chamber and the redox reaction in the cathodic chamber. In an anodic half-cell, the organic compound is exoelectrogenically, which is to say, the electrochemically active microorganism is capable of transferring the electron extracellularly (Logan, 2009). For a long time, this was thought to be impossible. To illustrate this, the reaction which occurs in the anodic compartment with a glucose substrate can be represented as below (Mahadevan et al., 2014):

$$C_6H_{12}O_6 + 6H_2O \rightarrow 6CO_2 + 24H^+ + 24e^- \quad (2.10)$$

Here, glucose catabolism releases 24 protons and 24 electrons into the extracellular environment. The bacterium arrives at the anode and donates an electron which travels through the external circuit to the cathodic chamber. Meanwhile, the proton will diffuse through the half-cell separator into the cathodic chamber where oxygen typically is used as the terminal electron acceptor due to its high redox potential (i.e., "+1.229 V"), limitless availability, and low cost. (Song et al., in press). The proton, electron, and oxygen react at the cathodic chamber to form water in an oxygen reduction reaction, which can be represented by:

$$6O_2 + 24H^+ + 24e^- \rightarrow 12H_2O \quad (2.11)$$

2.1.6 Electron transfer mechanism in MFC

The microorganism continuously undergoes substrate catabolism in MFC, liberating electrons and protons into the anodic compartment. The selectively permeable half-cell separator allows proton crossover to the cathodic chamber through proton gradient. The non-conductive structure of most microorganisms cannot transfer those electrons to the outside of the cell and

donate them to the anode. But electrochemically active bacteria or exoelectrogen are adapted to directly transfer an intracellular electron to the extracellular environment without the assistance of a mediator (Logan, 2009). This microorganism either developed a modified structure or synthesized particular molecules that aid electrons to relocate outside the cell membrane.

On the other hand, certain redox-active species could facilitate electron transfer outside of the cellular membrane for the electrochemically inactive bacteria. Such redox-active species refer to the mediator. Schroder (2007) defined the mediator as a species of chemical that must be soluble, has physical contact with the electrode, and possess a low reduction potential. Its potential should come as close as possible to the organic substrate in the anodic chamber as well. Regardless of the bacterial type employed in the MFC, there are only a few electron transfer methods. Those methods can be classified into direct electron transfer and mediated electron transfer (Schroder, 2007).

2.1.6.1 Direct electron transfer

Through a process called extracellular respiration, exoelectrogenic bacteria are capable of transferring electrons to the extracellular medium. C-type cytochromes are one of the redox proteins that facilitate this transfer, typically found in metal-reducing bacteria such as *Geobacter* and *Shewanella* (Shi et al., 2007 In brief, the cytochrome proteins utilize a cascade of membrane-bound complexes, with a solid terminal electron acceptor, in this case, is Fe (III) or Mn (III, IV). This direct electron transfer results in forming a monolayer of cell membrane or organelle on the electrode surface. The specific mechanisms behind these processes are not well understood. One recent study suggests that the electricity generated in MFC can be elevated by overexpressing the cymA gene, which facilitates cytochromes translation in *S. oneidensis* MR-1 (Vellingiri et al., 2019).

A major bottleneck in redox protein electron transfer is the total number of bacteria in the monolayer to contact the electrode (Torres et al., 2010). Some bacteria have evolved a conductive pilus, also known as a nanowire, to aid in extracellular respiration (Figure 2.6). Reguera et al. (2005) observed extracellular electron transfer in the C-type cytochrome-deficient species *G. sulfurreducens* via this faculty. One year later, another metal-oxidizing bacterium *S. oneidensis* had been reported to produce a nanowire as well (Yuri A. Gorby et al., 2006). The physiology of the microbial nanowire remains not fully understood. It is believed that the subunit-protein PilA, consisting of five aromatic amino acids, enables/controls electron transfer through the nanowire (Vargas et al., 2013).

Importantly, this nanowire structure significantly improves the overall efficiency of charge transfer to the electrode (Schroder, 2007). It acts as a conduit that allows a significantly increased number of bacterial cells to contact the electrode's surface area, leading to a thicker bacterial biofilm. Malvankar et al. (2011) calculated the conductivity of the nanowire to be:

$$\sigma = G(\frac{2a}{gL}) \tag{2.12}$$

where G is the bacterial biofilm conductance, 2a is gap width, L is the length of the electrode, and g is the thickness of biofilm; and they present a method for measuring G and g.

Extensive studies have been focused on two nanowire-producing bacteria *G. sulfurreducens* and *S. oneidensis* (Creasey et al., 2018). Beyond these, only a limited number of microbes capable of producing nanowires have been discovered. A broader search for nanowire-producing microbes is required to elucidate the genetic background and deepen our understanding of the electro-physiology of nanowires.

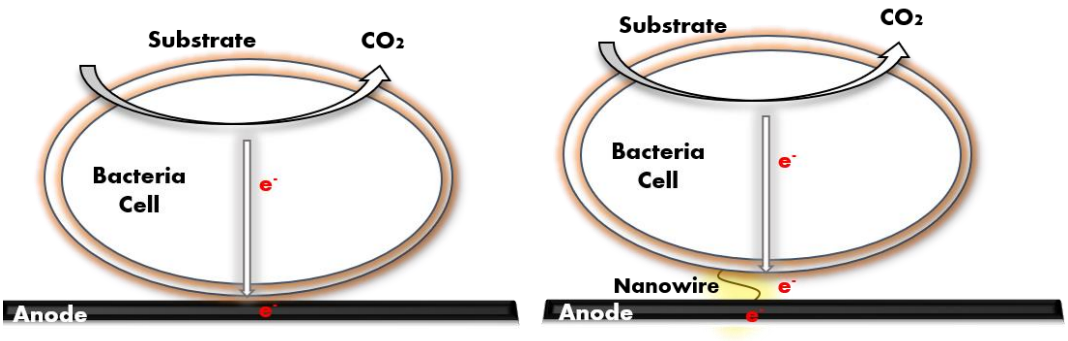

Figure 2.6 Direct electron transfer via membrane bound protein and via conductive nanowire structure

2.1.6.2 Mediated electron transfer

Most bacteria do not produce electrochemically active proteins or nanowires, in which case a mediator (or redox agents) is needed to facilitate electron transportation. This electrode-contactless method can achieve superior performance on substrate removal while effectively generating electricity (Uria et al., 2017). Two types present themselves: exogenous-mediated and metabolite-mediated (Schroder, 2007).

An exogenous mediator completes the external circuit between electrode and bacteria. Oxygen would be a superior mediator (because of its superior electronegativity), but the anaerobic

bacteria require a low-oxygen solution. A good mediator must be highly permeable to the bacterial cell; it must have a favorable overpotential to drive oxidization at the electrode; and ditto in its reduced form to lure electrons from the bacterial cell (Mahadevan et al., 2014). Specifically, the oxidized mediator must penetrate the cell, procure an electron, migrate back across the membrane, and give that electron to either the electrode or a terminal electrode acceptor. A schematic of exogenous-mediated electron transfer is provided in Figure 2.7.

Several exogenous redox mediator compounds have been investigated, including dyes such as methylene blue, natural red, resorufin, and thionine – as well as color-shifting inorganic compounds such as potassium ferricyanide (Emde et al., 1989; Rahimnejad et al., 2015).

While multiple studies have demonstrated the efficacy of redox mediators (Evelyn et al., 2014; Lohar et al., 2015), there are also intrinsic limitations posed by this method. For example, the requirement for continuous addition of mediator, the inability to penetrate thick biofilms, net economic inefficiency, and potential toxicity. In sum, exogenous mediation seems impractical for commercial and large-scale applications (Mahadevan et al., 2014).

Some microbes, however, have adapted to produce their own endogenous mediators by employing primary and secondary metabolites low-molecular shuttles. One example is *Pseudomonas spp.*, which excretes pyocyanin to serve as a shuttle/mediator (Rabaey et al., 2004), though at the cost of some ATP (Lovley, 2006).

Self-mediating bacteria present a competitive advantage under batch conditions in which the substrate is continually replaced. In such a system, a steady replacement of mediators is necessary. Sulfate/sulfide cycling is quite suitable for electron self-mediation, yielding a standard biological potential of -0.22V (Schroder, 2007). During respiration, the sulfate reduces sulfide; upon contact with the electrode, the sulfide oxidized to complete the cycle. Primary metabolites derived from fermentation and anaerobic respiration could assist this self-mediating process. An energy-rich reduced substrate (such as hydrogen and ammonia) is directly used as a mediator in fermentation. The energy-rich substance is oxidized by bacteria with the aid of the electrocatalytic anode – thereby avoiding the interruption of other biological processes (Schroder, 2007).

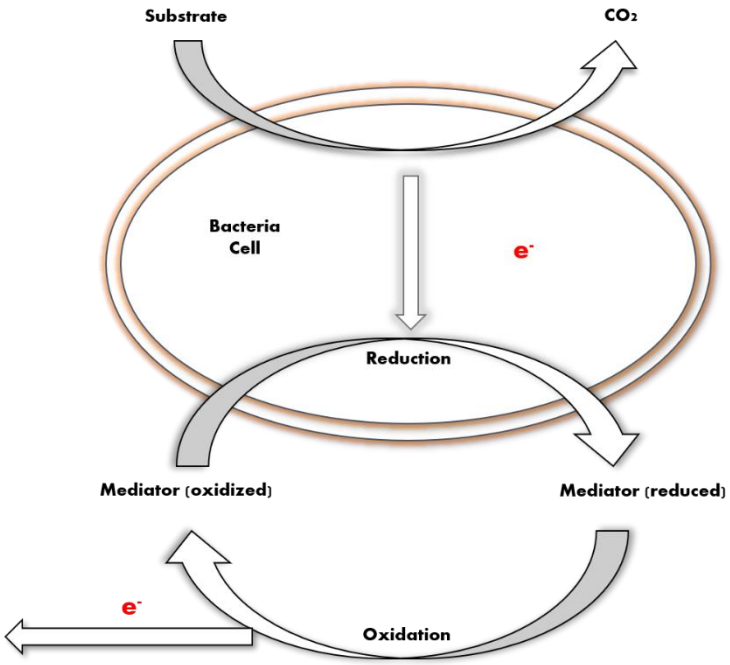

Figure 2.7 Illustration of mediated electron transfer within a microbial cell

2.1.7 MFC performance and optimization

Recently, intensive research has been focused on optimizing power generation through a multidisciplinary approach to MFC devices.

Carbon-based electrodes have drawn lots of attention because of their excellent biocompatibility, conductivity, and competitiveness. Surface area and porosity are essential to reduce internal resistance and ohmic losses (Kalathil et al., 2018). More recently, nanotechnology has led to the emergence of electrodes based on carbon nanotubes, which present a 3D nanostructure and large porosity and generate superior MFC (Delord et al., 2017).

Energy losses within the MFC are primarily due to three mechanisms: activation polarization (η_{act}), ohmic processes (η_{ohm}), and concentration polarization (η_{conc}) (Rismani-Yazdi et al., 2008). Activation loss dominates in the low current densities, where the initiation of electron transport must overcome the energy barrier of the reacting species. These losses may be mitigated by increasing the anodic surface area, introducing redox mediators, and increasing the operating temperature. (Mahadevan et al., 2014). Ohmic losses are caused by the MFC's internal resistance and can be easily calculated by ohm's laws. These losses can be reduced by shortening the distance between electrodes and employing better conductive material (Mahadevan et al., 2014). At high current densities, the incapability of maintaining the mass transfer rate of substrate/product results in an increase/decrease in the anodic/cathodic potentials. Concentration

polarizations occur when high current density and cell potential drop depart from the linear relationship with the current density profile. A longer growth time of biofilm on the anode could result in higher limiting current and fewer polarization losses when other condition remains the same (Zhao et al., 2014)

Collectively, the energy output of an MFC can be predicted by (Rismani-Yazdi et al., 2008):

$$V_{op} = E_{cell} - (\eta_{act} + \eta_{ohm} + \eta_{conc}) \quad (2.13)$$

2.1.8 Cell potential modeling -The Nernst equation

Microbial fuel cell models have been studied by Zhang and Halme (1995): an oversimplified model will lead to detail loss from MFC, and an overcomplex model will lead to higher difficulty in data analysis. Considerations must be made for biological, electrochemical, physical, and diffusive processes. Nonetheless, the redox reaction is considered as first-order reaction in the modeling by Zhang and Halme (1995):

$$E_{cell} = E_{cathode} - E_{anode} \quad (2.14)$$

The potential of the redox reaction of bacteria degrading the substrate in an anodic chamber is equal to the standard potential between two half-reactions. The standard cell potential can be calculated from the Gibbs free energy:

$$E_0 = \frac{\Delta G}{-nF} \quad (2.15)$$

Where ΔG is the Gibbs free energy, n is the number of electrons transferred during the reaction, and F is the faraday constant.

However, the cell's overall potential depends on the concentration of reducing/oxidizing agents and environmental factors. The Nernst equation accounts for these effects (Feiner & McEvoy, 1994):

$$E_{cell} = E^{\emptyset}_{cell} - \frac{RT}{n\mathrm{F}} \ln Q_r \quad (2.16).$$

Where R is the universal gas constant, T is the temperature in Kelvin, n is the mole of electrons, and Q_r is the reaction quotient, defined as the relative amounts of product and reactant present during the reaction at particular time. For example, for the reaction:

$$aA + bB \rightarrow cC + dD \quad (2.17)$$

The reaction quotient, Q_r, is defined as:

$$Q_r = \frac{[C]^c[D]^d}{[A]^a[B]^b} \quad (2.18)$$

Additionally, other biological processes, including complex enzyme reactions and microbial growth in the fuel cell, are highly dependent on substrate availability. Such process can be modeled by Monod-type kinetics (Kovárová-Kovar & Egli, 1998):

$$\mu = \mu_{max} \frac{[S]}{K_s + [S]} \tag{2.19}$$

Where μ is the growth rate, S is the concentration of substrate, and K_s is the half-velocity constant.

Two diffusive processes occur in the fuel cell: hydrogen ions diffuse through PEM into the cathodic chamber and external oxygen from diffusing/dissolving into the catholyte. Those processes can be modeled by Ficks' second law of diffusion (Paul et al., 2014). However, Zhang and Halme (1995) demonstrated that the diffusion process is fast enough to affect neither cell potential nor power generation and can thus be neglected under normal circumstances.

2.1.9 Electrochemical biosensing and MFC-based biosensor

Sensors in modern industrial applications cover the entire spectrum of input parameters converted to an electrical signal. In recent years, the strong demand for real-time, on-site, simple, cost-effective designs has led to the use of biosensors in fields as diverse as pharmaceuticals, medical applications, foods, and the environment.

The majority of biosensors operate either enzymatically or electrochemically. Enzymatic biosensors have the advantages of specificity and high sensitivity yet suffer from complex preparation protocols and a short lifetime (Mulchandani, 1998). On the other hand, an MFC-based biosensor is an electrochemical approach. It is a versatile tool, sensitive to a large variety of analytes, and offers a simplified preparation protocol, sustainable and cost-effective at scale. As such, it is a viable future alternative for enzymatic biosensors (Su et al., 2011).

An MFC device generates an electrical signal that effectively monitors microorganisms' metabolic activity kept under steady-state conditions. The microorganism within the anodic compartment acts as the recognition agent that responds to any alteration (pH, solution concentration, specific compound) in the environment, affects the flow rate of electrons of the external circuit, and transduces into a measurable voltage signal. Thus, any environment disturbance results in a change in voltage/ampere, making the MFC an *in-situ* biosensor (Cui et al., 2019). Any fluctuations are securely coupled to the redox reactions within the MFC – an advantage not available to other types of amperometric biosensors (Lovley, 2008).

In an unsaturated anodic solution, the change of concentration of biodegradable substrate will directly affect the metabolic rate of microorganisms and, consequently, the flow rate of the

electrons and the signal output. This approach is mainly used for *in-situ* environment monitoring for labile carbon such as BOD, COD, or toxic carbon monoxide (Peixoto et al., 2011; Zhou et al., 2018). On the contrary, in a saturated and steady anodic environment with constant external factors, a sudden change of the MFC biosensor's signal output may be caused by the emergence of a new bioactive compound within the feed stream. This approach is mostly used to detect toxic components in water (Chouler & Di Lorenzo, 2015), as the inhibition of microbial activity reduces the amount of electricity generated. This technique is favored by the wastewater treatment industry as it can detect and prevent four major types of toxicant discharge, including heavy metals, antibodies, and organic and acidic toxicants (Cui et al., 2019). It is important to note that the toxicant concentration may exceed the detection range of MFC biosensor; therefore, the sensitivity of the microbe(s) vis-à-vis the inhibition effect of the toxin are important pre-considerations. Sensitivity is defined as the electrical signal change per unit change of concentration of target analyte:

$$Sensitivity = \frac{\Delta I}{\Delta c * A} \tag{2.20}$$

where ΔI is the change in current output, Δc is the change in the target analyte concentration, and A is the anode surface

(Di Lorenzo et al., 2014). The inhibition effect can be calculated by modified Michaelis-Menten Equation:

$$I(\%) = \frac{|CY_{nor} - CY_{tox}|}{CY} * 100 \tag{2.21}$$

Where CY is the coulombic yield and is obtained by integrating the electrical signal generation over time, and CY_{nor} and CY_{tox} are the coulombic yields in normal and toxic conditions.

Furthermore, the MFC-based biosensor could be used as a monitor for microbial dynamics. Liu et al. (2011) utilized an MFC-based biosensor to monitor the anaerobic digestion of a microbial consortium in a wall-jet MFC with varied feedstock concentration and process configuration. The MFC biosensor signal presents a clear correlation between signal and various parameters. A recent study shows that by incorporating high-throughput Illumina® sequencing technology with the voltage generated by an MFC bioreactor one could successfully monitor the microbial community growth dynamics (Pepè Sciarria et al., 2019).

So long as the details of the bacterial mechanisms remain elusive, most research continues to focus on bacteria-consortia of the naturally occurring environment or of industrial wastewater

(Vejarano et al., 2019). So far, real-world implementations of MFC biosensors have been limited to these consortia or to single microbial strains.

2.2 Knowledge gap

Historically, the fermentation process can be monitored by microscopical presence, counting microbial population, or measuring the level of a key metabolite in the fermenter. Such monitoring techniques can easily be accomplished without specialized skills and equipment. In recent decades, the rapid development of bioelectrochemical technology and the emergence of digital sensors enable a more effective and precise fermentation monitoring process. ORP measurement by utilizing the ORP sensor is one of the most popular fermentation monitoring and control approaches. Such a method provides an online and consistent signal during fermentation. It also can be used in any stage of operation, providi ng high signal integrity and measurement reliability. However, the high fabrication cost of an ORP sensor and instrumentation makes it impractical for large-scale applications in industrial fermentation. Cost-effectiveness is an endless effort in engineering study, and an economically optimized ORP monitor tool is urgently needed.

MFC is an electrochemical system. It utilizes an active microorganism as the biocatalyst for bioelectricity production. Besides power generation, it can be used as a tool as a biosensor. Most MFC-based biosensor research focuses on an environmental study, such as detecting the substrate concentration or the presence of the substance of interest in the environment. Furthermore, the Nernst equation provides a relation to associate the signal output from an MFC device with the level of redox potential from microbial activities. Valiadation of such correlation derived from Nernest equation under actual MFC conditions is nececarry for the development of fermentation process equipped with MFC-based biosensors.

.

2.3 Hypotheses and objectives

The following hypotheses will be tested as a part of this research:

- The microbial growth stage is associated with the signal output from an MFC device.
- The voltage output presents a correlation with ORP level within an MFC device.
- The correlation between voltage output from an MFC device and redox potential level from an ORP sensor could be used to monitor the progress of a fermentation process.

The purpose of this study is to establish a cost-effective approach for a large-scale fermentation process that is capable of real-time monitoring strategy by utilizing an MFC device as an ORP sensor. The specific objectives include:

- To correlate a relationship among voltage output, redox potential within MFC and microorganism growth stage.
- To develop a new approach for fermentation monitoring by biosensing technology.

3 MATERIALS AND EXPERIMENTAL METHODS

3.1 Strain and cultivation

Bacillus. subtilis is a commercial bacterial strain isolated in Taiwan (Yanten Biotechnology Co., Ltd.). Our growth medium was a modified Lysogeny broth (LB), consisting of peptone 10g/L, NaCl 10g/L, yeast extract 5g/L, $MgSO_4$ 2g/L, and 1M NaOH 1 mL/L. The medium was sterilized at 121°C for 50 minutes prior to use. For long-term strain preservation, the modified Lysogeny broth was mixed with 20% glycerol and stored in a -80°C freezer.

Frozen seed culture of *B. subtilis* from the -80°C freezer was thawed and inoculated into 50 mL of modified LB broth with the addition of 15g/L of glucose. After incubation on the shaker bed (180rpm) at 25°C for 12 h, the regenerated culture was inoculated into a sterilized 250 mL beaker filled with 230 mL modified LB broth and incubated on the shaker bed at (180rpm) at 25°C for another 24 h.

Pseudomonas fluorescens local strain, ICW1057, was isolated from an oil-impacted field from Saskatchewan, Canada in our lab (Huang & Lin, 2020). This strain will be used as a comparator to *B. subtilis* in order to evaluate their respective performance in MFC device. A modified minimal salt medium is used for bacterial replication and incubation. The minimal salt medium is sterilized at 121°C for 50 minutes prior to use. All chemicals used in strain cultivation and replication were obtained from VWR International (Edmonton, AB, Canada) and Fisher Scientific (Ottawa, ON, Canada).

3.2 Microbial fuel cell-based biosensor design and construction

The MFC-based biosensor is designed based on a double-chambered MFC device, which is most easily controlled and modified in the laboratory environment. A proton exchange membrane located at the middle dividing the device into anodic and cathodic compartments. The microbial fermentation process is carried out at the anodic chamber, and the reduction process is conducted at the cathodic chamber. Two low-cost graphite rods are employed as electrodes and inserted into each respective compartment. The anodic chamber is equipped with an ORP probe for environmental redox potential detection. Two air pumps connect to each compartment to control the aeration rate and oxygen level. A pH regulation system is also connected to the anodic chamber to prevent fluctuation of redox potential triggered by pH change. The anode and cathode are connected to an external circuitry for voltage signal detection and data collection. The

schematic of the experimental setup is illustrated in Figure 3.1., and specific construction materials and the experimental procedure are followed:

A standard H-shaped, two-chamber MFC with a 250 mL reactor (Wenoote Inc, China) and a 5cm-diameter PEM (Nafion 117, DuPont, USA) was used. The PEM was subjected to a three-stage pre-treatment (Ghasemi et al., 2013): first, immersed in 80°C water for 30 mins; second, immersed in an 80°C solution of 3% hydrogen peroxide; and finally immersed in 0.5M sulfuric acid. Subsequently, the PEM was rinsed with deionized water three times and stored in 0.5M hydrochloric acid. Both electrodes were graphite rods, 6mm in diameter and 100mm in length. The projection area of each rod was approx. 1725mm^2 (90mm length and bottom surface submerged). Rods were pre-treated by baked at 300°C for 20 minutes to remove impurities, soaked with acetone and methanol successively, and finally washed with deionized water three times.

The anodic chamber was inoculated with 24 mL of the *B. subtilis* and *P. fluorescens* (O.D. adjusted to 2.0-2.4), along with 226 mL of modified LB used as substrate (adjusted initial O.D. of anolyte between 0.2-0.24). The pH of the substrate was adjusted to 8 with 1M NaOH or HCl solutions, and a peristaltic pump was connected to the anodic chamber to maintain this pH throughout the operation. The cathodic chamber was filled with 240 mL distilled and deionized water. An air pump (Tetra Inc., China) was connected to each chamber for sparging. A gas flowmeter (SHO-RATE, Brook instrument CO., USA) was maintained an aeration rate of 0,11.32, and 22.64 vvm in the anodic chamber, while flowrate through the cathodic chamber was kept over 10 gallons/min without control. A bottle of deionized water and air filters were connected between the air pumps and each chamber to provide humid and sterile sparging condition in order to prevent electrolyte evaporation. Additionally, a disk-shaped stir disk was placed in the anodic chamber, and the MFC was placed on a stir plate (110rpm) to allow air to dissolve into the anolyte evenly. An external 324 kΩ resistor was connected across the anode and cathode with titanium wire. Both ORP and pH sensors (Van London Co., USA) were inserted into the anodic chamber for data acquisition. All components of this apparatus were sterilized in an autoclave at 121°C for 50 minutes before use.

Additionally, the effect of the supplement of mediator and catholyte had been tested in this set of experiments, where 1% 1M of methyl blue was added into the anodic chamber to facilitate the electron transfer. Also, 1% 1M potassium ferricyanide was added into the cathodic chamber as an alternative for oxygen as terminal electron acceptor.

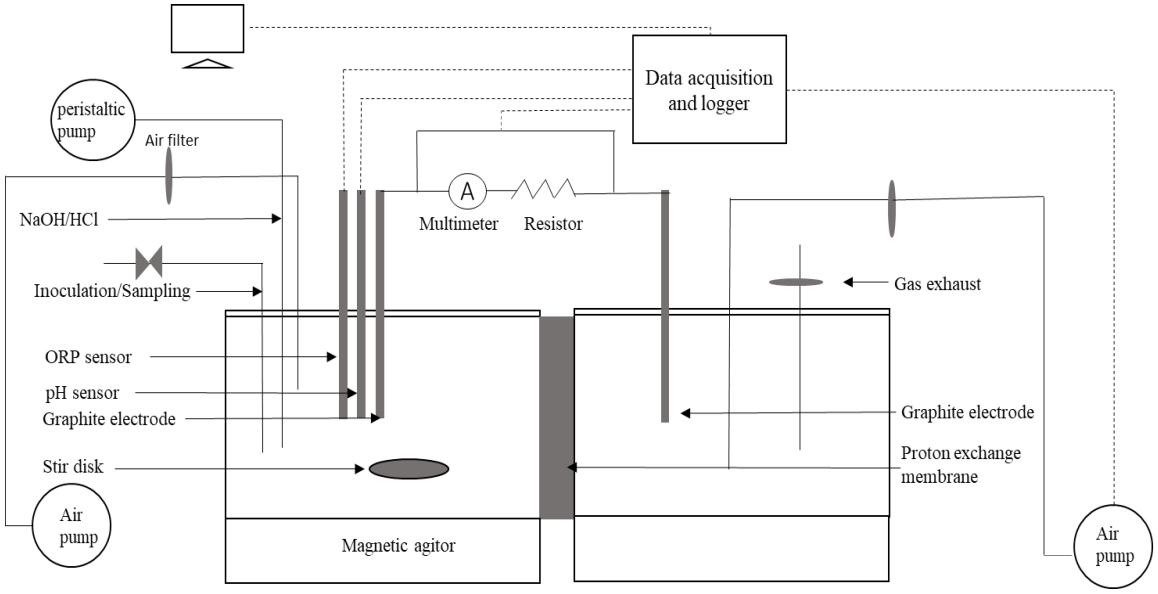

Figure 3.1 The MFC apparatus diagram

3.3 Analytical procedures

The electrical voltage across the resistor was measured by the Phidgets VINT hub (Phidgets Inc, Canada) and recorded using a computer-based data acquisition system (National Instruments, LabVIEW, version 19.0f2) at 10s intervals. The current was calculated by Ohm's law**:** I=V/R.

The redox potential measurement used an ORP sensor connected to a pH/Temperature/mV/ISE multi-meter (VWR Scientific, USA). The data was recorded by the computer-based data acquisition system mentioned above at 10s intervals.

Biomass concentration was determined based on the optical density (OD_{600}). The bacterial suspension within the anodic chamber was sampled every hour after the 5-hr lag period. Each sample was withdrawn with a 5-mL sterile medical syringe and tested for optical density and biomass change by a benchtop spectrophotometer (UVmini-1240, Shimadzu Inc, Japan) of 600nm wavelength.

4 RESULTS AND DISCUSSION

The motivation of this research was to prove the concept of an alternative ORP measurement method and to design a prototype of an actual MFC-based fermentation sensor. Different factors, including microbial types, fermentation conditions, and environmental factors, were considered in this work. The results were broken down into a few parts, including testing two types of microorganisms with or without the supply of artificial electron mediator, using different catholyte and catholyte treatments, applying different anodic chamber aeration rates, and analyzing the ORP change, voltage output, and (unitless) potential parameter that we derived from the Nernst equation, respectively.

4.1 Modification of the Nernst equation for MFC application

The Nernst equation is well established and had been proven by a large amount of experimental evidence. This equation can be derived directly from basic thermodynamic principle and applied to two major cases, including the equilibrium potential of an electrode (redox electrode or metal ion electrode) in a Galvanic cell and the potential (voltage) of a cell reaction of an electrochemical cell (Scholz, 2017). In this experiment, the redox potential and voltage of the microbial fuel cell are both subjected to the Nernst law. The Nernst equation is applied to our work and can be described as in Equation 3.1:

$$\boldsymbol{E_{cell} = E^{\emptyset}_{cell} - \frac{RT}{n\mathrm{F}} \ln Q_r} \qquad (3.1)$$

Where the E_{cell} is the actual cell potential, $E^{\emptyset}_{cell}$ is the theoretical cell potential, R is ideal gas constant, T is temperature, *n* is the number of electrons, F is faraday constant, and Q_r is reaction quotient that represents stoichiometric measurement of relative amounts of oxidant and reductant of the redox reactions in the MFC devices.

By moving the $E^{\emptyset}_{cell}$ to the left side of the equation, the change of the cell potentials within the MFC could can be calculated by:

$$\boldsymbol{E_{cell} - E^{\emptyset}_{cell} = -\frac{RT}{n\mathrm{F}} \ln Q_r} \qquad (3.2)$$

Where the $E_{cell} - E_{cell}^{\emptyset}$, is change of the initial cell potential and in the MFC-based fermentation reaction, and the redox potential is a quantitative indicator of the degree of completion of the biochemical reactions. In this case, the difference between E_{cell} and $E_{cell}^{\emptyset}$ can be consider as the change of redox potential in the MFC:

$$\Delta \boldsymbol{ORP} = -\frac{\boldsymbol{RT}}{nF} lnQ_r \quad (3.3)$$

Where $-\frac{RT}{nF} lnQ_r$ is equal to the change of the redox potential in the MFC device, Q_r is the reaction quotient that represents the stoichiometric balance of oxidants and reductants involved in the MFC-based fermentation. However, fermentation consists of a series of complicated redox reactions, and many intermediate products and derivatives are formed. In this case, we could assume that the oxidant is equal to the reductant with the electron activities. And the ultimate goal of all those transformations and conversions of chemicals and matters is for microbial cell metabolism and propagation. Hence, the Q_r is a unitless term that reflects matter exchange between a microbial strain and biomass gain during the course of fermentation and is conclusively called potential parameter X. As $\ln Q_r$ is a constant, the RT/nF represents an electric voltage measured in an MFC device and its unit is V or mV. This voltage is generated by the electrons that emit from the redox reactions during fermentation and is captured by the MFC device. Hence the RT/nF can be considered as the electron movement between anodic and cathodic compartment, consequently resulting in the voltage production from the MFC device (ΔV):

$$\Delta \boldsymbol{ORP} = -\Delta \boldsymbol{V}\, ln\, \boldsymbol{X} \quad (3.4)$$

Reorganized the Equation 3.4:

$$\boldsymbol{X} = \boldsymbol{e}^{-\frac{\Delta \boldsymbol{ORP}}{\Delta \boldsymbol{V}}} \quad (3.5)$$

Where the ΔORP is the change of redox potential from the microbial fermentation in anodic chamber, ΔV is the voltage between the anode and cathode. Because parameter X is a constant that correlated two potentials in the MFC device (ORP and voltage), it is named as potential parameter X.

Equation 3.5 demonstrates a relationship that could correlate the redox potential reading and voltage detection from the MFC device. Integrating such a relationship with the bacterial growth dynamic makes it possible to monitor and control the fermentation process.

4.2 Effect of different microorganisms on MFC-based biosensor performance

In this project, pursuing maximum electricity harvesting was not a priority. Biosensor research emphasized sensitivity, stability, and reliability instead. Due to the complex interactions in the microbial consortium, this study only examined the performance of the pure culture of bacteria. Two pure cultures of different bacterial strains, *Bacillus. subtilis*, and *Pseudomonas fluorescens* were the candidates for the MFC-based biosensor, and both performances with mediator presence or absence were examined in this section. Figure 4.1 showed the plots of voltage production and power density with the addition of a 0.1M methylene blue mediator. For *P. fluorescens*, it was observed that without the supplement of mediator, the voltage and power density occurred after the 8 h of fermentation and sharply climbed to 0.02V and 700 $\mu W/m^2$, respectively. Both values then gradually reached a peak around 30 h, giving out a maximum voltage production of 0.04 V and maximum power density of 2602 $\mu W/m^2$. The voltage and power density started to descend slowly until the end of fermentation. For the methylene blue addition group, the first signal appeared after 10 h of the experiment, and a rapid increase from 10 h to 15 h was observed. After that, both changes of voltage and power density became stable, and a comparatively slight increase until 48 h were observed. The maximum voltage was around 0.11V, and the maximum power density was around 17000 $\mu W/m^2$. For *B. subtilis*, without the supplement of mediator, the first voltage and power density produced at 6 h of fermentation, and the voltage and power density increased from 0 to 0.16 V and 63000 $\mu W/m^2$, respectively, from 6 h to 10 h of fermentation. Both values then remained stable until the end of fermentation, which gave out 0.19 V maximum voltage and 69356 $\mu W/m^2$ maximum power density. For *B. subtilis* with the mediator, the voltage and power density curves presented a similar pattern to the no mediator counterpart. Noticeably, *B. subtilis* with mediator generated the voltage and power density at the 3 h, which was the quickest among all four groups.

Regardless of the addition of the mediator, *B. subtilis* outcompeted the voltage and power production from the *P. fluorescens.* The *Pseudomonas* family, such as *P. aeruginosa* and *P. alcaliphila*, has been proven to be successful electrogens (Yong et al., 2011); however, the scientific community hardly investigated the *P. fluorescens'* electricity harvesting ability and its physicochemical properties in MFC. By comparing two plots of *P. fluorescens* without the aid of a mediator, the voltage and power density produced from this strain (*P. fluorescens*) presented discontinuousness and instability. The acceleration (8-13 h), deceleration of increase (14-32 h),

and acutely decreased phase (after 35 h) of the signal can be observed. A possible explanation for this performance might be that *P. fluorescens* lacked a shuttle to transfer the electron to the intercellular environment efficiently. Only a trace number of electrons can be released into the anodic chamber and detected by the electrode. When the mediator was added, *P. fluorescens* produced relatively higher voltage and power density because the methylene blue facilitated the electron shuttle to complete the half cell reaction.

Moreover, the voltage became stable around 20 h (Figure 4.1a), with average voltage production below 0.1 V, which presented a weak power generating ability for *P. fluorescens*. For B. *subtilis,* the similar pattern of voltage and power density generation regardless of the addition of mediator elucidated that *B. subtilis* was capable of producing sufficient shuttle to transfer the electron from intracellular to the extracellular environment. Nimje et al. (2009) examined the performance of *B. subtilis* in MFC. They proved that *B. subtilis*, which produced active and soluble redox compounds, could facilitate the extracellular electron transportation for MFC reactions. The electrochemical activity of *B. subtilis* was governed by the excreted metabolites redox compound, which reflexed the intercellular homeostasis and ORP balance. Furthermore, the endospore structure helped *B. subtilis* to overcome the environmental stress and to regulate the cell germination, which accelerated the cell multiplication phase and shortened the lag phase of bacterial growth (Mckenney et al., 2013). Additionally, the biofilm-forming adaptation of *B. subtilis* allowed fast sensing and constructed a stable communication between bacterial cells and anode (Ismail & Jaeel, 2013). In the presence of mediator, *B. subtilis* was able to produce power at 3 h of operation, contributing to the fast and thriving growth habitat; the bacterial cells reached enough population and carried out normal catabolism to liberate electrons in the substrate. Furthermore, the delayed emergence of power when *B. subtilis* without the addition of mediator may be caused by the biofilm and redox compound that can not be formed in the early fermentation stage.

P. fluorescens lacked an endogenous method to shuttle electrons and required an external mediator for electron transfer. The insufficient or exceeded addition of mediators would lead to the adverse effect on bacteria themselves and inaccurate MFC sensing response (Mohan et al., 2007), which caused more serious operational difficulty and economic cost. Furthermore, *B. subtilis* presented a significantly shorter period for cell multiplication. The growth-promoting feature and the fast-building bacterial colony enabled the biofilm formation and robust growth of

bacterial cultures. Considering the sensitivity of bacteria, life cycle, and bacterial behavior, *B. subtilis* presented superior performance as an MFC-based biosensor experiment candidate.

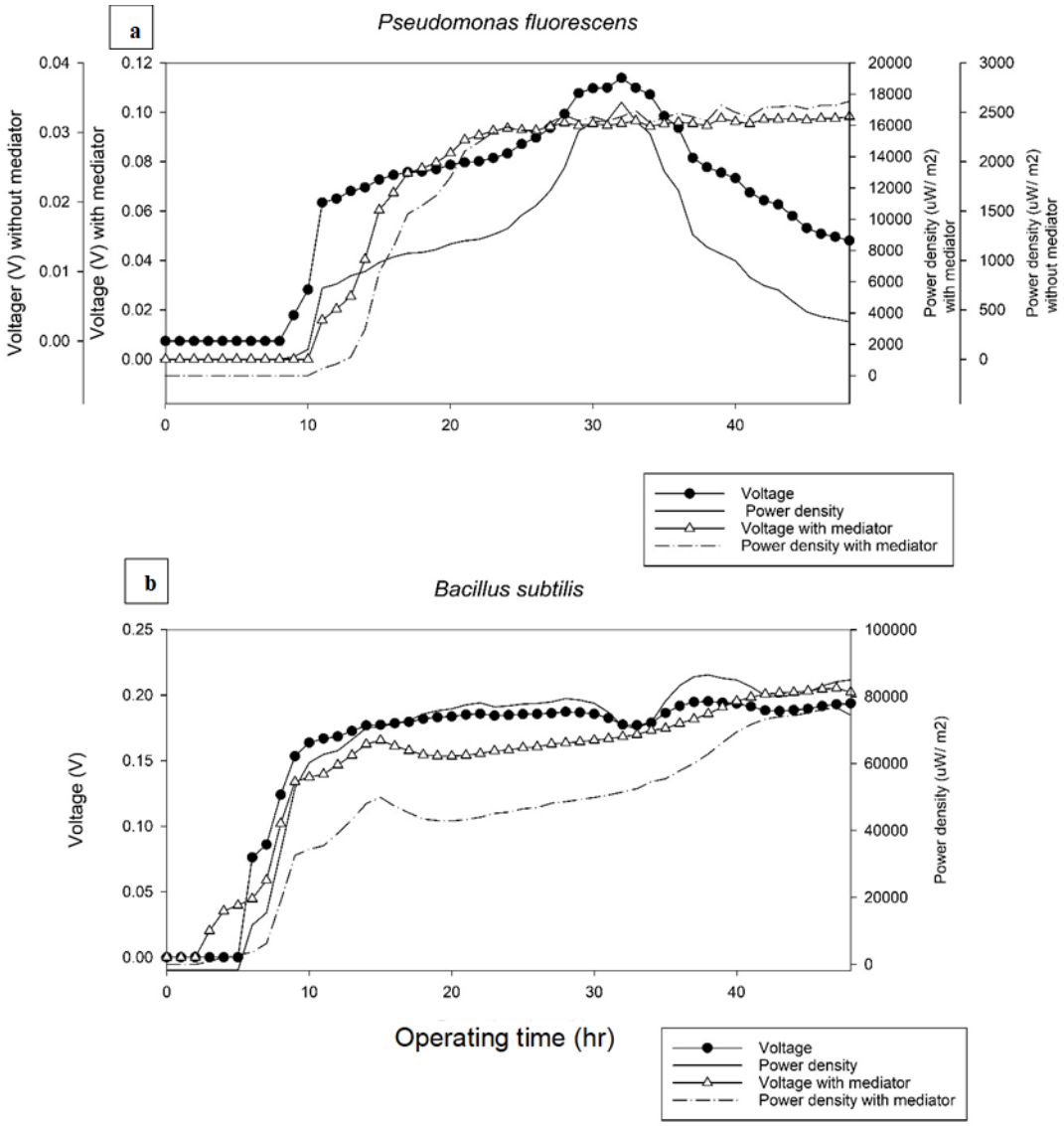

Figure 4.1 Voltage production and power density of two different bacterial strains over 48 h. fermentation.

4.3 Effect of catholyte and catholyte treatments on the MFC-based biosensor performance

As an important part of MFC, cathodic compartment was to provide a confined space and to serve as terminal electron acceptor to complete the fuel cell half-reaction. Oxygen is a ubiquitous electron acceptor used in the cathodic chamber due to its low cost and high oxidation potential. Another alternative approach is using a high oxidative chemical compound. Furthermore, oxygen

in the air can be directly used by an air cathode, but construction and well-conducted air-cathode require costly catalysts and material (Kakarla et al., 2015). Based on the scope of the MFC-based biosensor, this section compared a sparged air cathode and a potassium ferricyanide solution cathode, and a simple aerated cathode was used as the control group.

In Figure 4.2, the voltage produced from the three groups (sparging treatments, potassium ferricyanide catholyte, and aerated cathode) has been plotted. The potential generated from aerated cathode around 6 h after inoculation, and the potassium ferricyanide catholyte voltage developed at 7-8 h after inoculation. Sparging treated group signal appeared at 9-10 h of operation. All three groups' voltage increased until around 20 h, and the air cathode voltage production suddenly dropped to 0 at 22 h. The voltage from the potassium ferricyanide group kept a sharp increase until 24 h. The increment became more gradual around 24-46 h, and a maximum voltage around 0.21 V was observed. The voltage decreased slightly afterward and was stable around 52-53 h, with a final voltage around 0.2 V at the end of the experiment. The sparging group had significant growth of voltage production until 20 h, and then the slope became flat from 20-40 h. A peak occurred around 42 h with 0.14 V maximum voltage generation. Then the voltage started to decrease and remained stable until the end of fermentation with approximately 0.13V. The air-cathode MFC had lower internal resistance than MFC with ferricyanide.

Each cathode treatment exhibited rapid start-up, but the potential generated by the aerated cathode group vanished and could not provide a stable signal over a long period of time. This may be due to the dissolved oxygen in the catholyte being quickly consumed by electrons and protons emitted from the anodic compartment. As the oxygen was exhausted in the cathodic chamber, there was insufficient electron acceptor to the support fuel cell half-reaction. More importantly, the oxygen dissolution and diffusion rate into the catholyte was much lower than the consumption rate from the fuel cell. After oxygen depletion, every oxygen molecular was dissolved into a cathodic chamber, quickly offset electron accumulated in the circuit, which resulted in minor potential difference to overcome the internal resistance for proton transportation. Eventually, voltage sharply dropped to and remained at 0 after oxygen depletion.

By comparing the sparging and potassium ferricyanide catholyte, the potassium ferricyanide exhibited superior overall power and voltage production than the sparging group. The difference in power generation may be attributed to the different types of electron acceptors. Lawson et al. (2020) reported that when the electrode resistance was similar for ferricyanide and

oxygen as the electron acceptor, the ferricyanide carried a more significantly experimental working potential. When utilizing oxygen as the electron acceptor, the half-reaction at cathode would be, and the theoretical potential can be calculated by Nernst equation:

$$E = E^{\emptyset} - \frac{RT}{4F} ln \frac{1}{[O_2][H^+]^4} \quad (3.6)$$

On the other hand, the half-reaction of potassium ferricyanide would be $Fe(CN)_6^{3-} + e^- \rightarrow Fe(CN)_6^{4-}$, the corresponding potential is:

$$E = E^{\emptyset} - \frac{RT}{F} ln \frac{Fe(CN)_6^{4-}}{Fe(CN)_6^{3-}} \quad (3.7)$$

The oxygen possed a higher redox potential of 1.23 V, and ferricyanide had a lower redox potential of 0.36 V. However, when utilizing oxygen as an electron acceptor, the actual cell potential was exhibited an exponential relationship to oxygen concentration, which consequently caused the cathode polarization. In contrast, the potassium ferricyanide contributed to the cell potential by the concentration of ferricyanide. Using the potassium ferricyanide as the electron acceptor led to a faster reduction rate and higher voltage production when there was much lower overpotential and higher solubility within potassium ferricyanide (Ucar et al., 2017). Oh and Logan (2006) reported a similar result, 1.5-1.8 times of increased power production in MFC was observed when the ferricyanide was used as electron acceptor.

In contrast to the power production-oriented MFC, signal clarity, real-time response, and stability emphasized the MFC-base sensor. Besides the voltage production, both the sparging group and potassium ferricyanide group were comparable in producing stable, clear, and similar voltage signals. Using non-sustainable potassium ferricyanide as a catholyte could increase the operational cost and difficulty and also could make the MFC biosenosr less productive. The aerated cathode required minimum attention, but the oxygen diffusion rate in the cathodic chamber is much lower than the electron production rate in the anodic chamber. After the existing oxygen molecule is exhausted, the voltage drop to zero. Although the oxygen is continuously diffused into the catholyte, the trace amount of oxygen is suddenly consumed by the half-reaction, and there is no detectable voltage signal generated due to there is not enough power density to overcome the overpotential for activation polarization. All these results suggested that the sparging group could be the optimal cathodic treatment for this MFC-based biosensor.

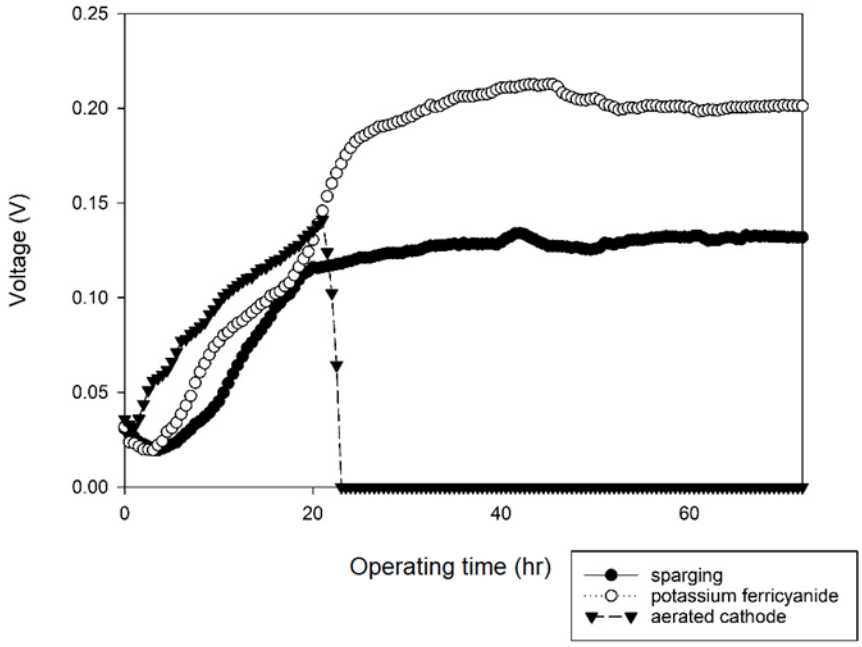

Figure 4.2 Comparison of voltage signal generation among three different electron acceptor sources and treatments in cathode.

4.4 Effect of aeration in the anodic chamber on the MFC-based biosensor performance

To investigate the effect of the growth of *B. subtilis* under semi-aerobic or anaerobic conditions on the MFC-base biosensor performance, the voltage production and ORP change under different aeration rates in the anodic chamber were tested. As presented in Figure 4.3, the left scatters chart portrayed the voltage generated from the MFC device. The plot on the right side showed the ORP change over time in the anodic chamber under no aeration, aeration at 11.32 vvm, and aeration at 22.64 vvm aeration condition, respectively. To eliminate technical variability and convenience for visualizing the data, both voltage and ORP were normalized. What stands out in the figure was that the voltage generated from the 11.32 vvm outcompeted the other two groups with two folds of voltage. For the 11.32 vvm aeration group, there was a steep rise from 2 to 8 h of operation. After that, the voltage leveled off from 9 to 16 h. Another noticeable increase of voltage appeared from 20-40 h. For the no aeration group, the voltage production showed a sharp rise in the first 5 h of fermentation, and then the curve gradually increased from 5-50 h, followed by the a slight drop at the end of the experiment. In the 22.64 vvm aeration group, the voltage increased gradually almost during 72 h of experiment, with only a slight drop observed in 30 h. Regarding ORP, all three groups expressed a similar pattern of change. The ORP markedly declined in the first 10-12 h and gradually decreased over time. However, closer inspection of the

figure showed that the no aeration group ORP dropped significantly after 12 h, but the ORP started to increase when the experiment was near the end.

For a long time, *B. subtilis* has been widely considered as a strict aerobe. At the end of the last century, the aerobic growth habitat of *B. subtilis* was identified, and specific genes that could facilitate anaerobic respiration were isolated by several studies (Glaser et al., 1995; Nakano et al., 1997; Nakano & Zuber, 1998). As the present study was designed to determine the effect of semi-aerobic or anaerobic anodic environment on the MFC-based biosensor, different aeration rates were introduced to the experiment. Among three different aeration groups, the 22.64 vvm aeration group presented the lowest voltage generation. This low voltage generation could be attributed to the exceeded oxygen that remained in the anodic environment. And exceeded oxygen act as the electron acceptor to complete the half cell reaction that was supposed to happen in the cathodic chamber, which adversely affected the voltage production of the MFC-base biosensor. Furthermore, the voltage curve from the 22.64 vvm aeration group presented a near-linear increase and then flat growth, and the sensitivity of the biosensor may also be affected by the high aeration rate. Kolodkin-Gal et al. (2013) have demonstrated that high oxygen levels triggered the regulatory pathway and inhibited *B.sbutilis* synthesis of extracellular matrix. Similar observation were also seen in this study. A high aeration rate in the anodic chamber impaired the biofilm formation, leading to MFC carrying lower efficiency in electron transfer and lower sensitivity. When comparing to no aeration and the 11.32 vvm groups, both voltage curves presented a similar pattern, except that the 11.32 vvm group showed a more significant change in the voltage. As mentioned above, the exceeded electron acceptor in the anodic chamber would cause low efficiency of electron transfer rate to the cathodic chamber and led to a lower potential difference. A possible explanation for the more significant change of voltage in 11.32 vvm group might be that *B. subtilis* was both active aerobic and anaerobically, but anaerobic growth of *B. subtilis* presented a weak population multiplication and electron-producing ability. Nakano and Zuber (1998) reported that *B. subtilis* undertook either nitrate respiration or fermentation under strictly anaerobic conditions, and when oxygen was limited, this strain used nitrate or nitrate as a terminal electron acceptor instead. Nevertheless, nitrate respiration led to poor growth of bacteria and loss of the ability for sporulation (Hoffmann et al., 1995). The ORP result further supported the idea of anaerobic respiration. In the no aeration growth, the ORP in the anodic chamber sharply decreased as the nitrate in the substrate was quickly consumed. As the population reached the maximum capacity,

both voltage and ORP change were changed gradually. Near the end of the experiment, after the nutrient in the substrate was exhausted, *B. subtilis* started to die, and organic matter was degraded back into the environment. The voltage began to decrease while the ORP started to increase correspondingly. In a nutshell, both no aeration treatment and 11.32 vvm aeration treatment on the MFC anodic chamber provided suitable growth conditions for bacteria and supported the MFC-based biosensor functions. For 11.32 vvm aeration rate treatment, a suitable oxygen supplement supports the vigor growth of *B.subtilis* in the anodic chamber, no excessive oxygen to jeopardize the voltage production, and exhibits fewer disturbances during the 72-hour experiment cycle. Hence, the 11.32 vvm aeration rate in an anodic chamber was more feasible for utilizing *B. subtilis* in an MFC-base biosensor.

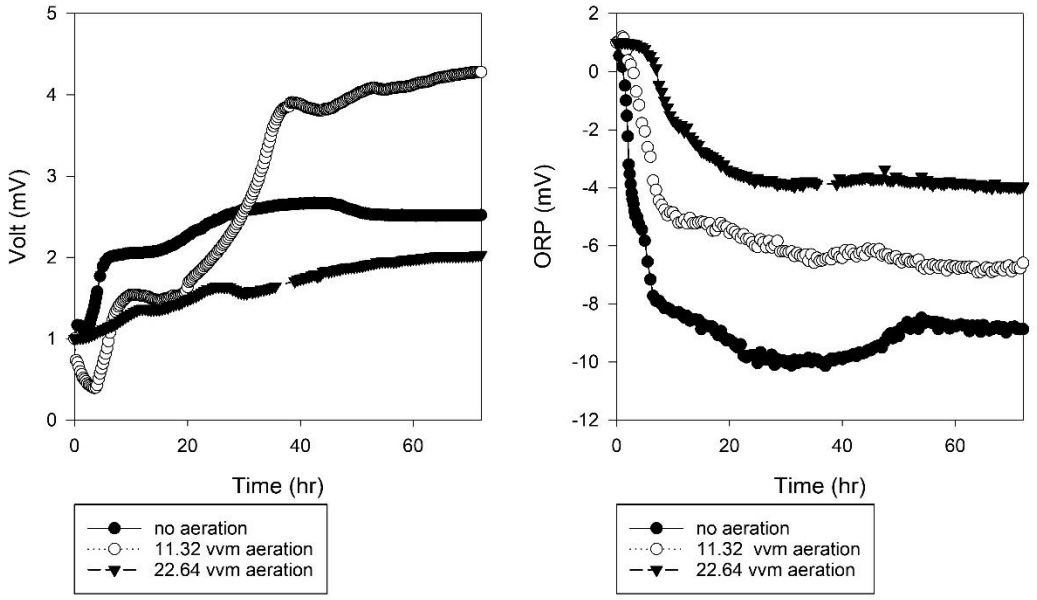

Figure 4.3 The effect of three different aeration rate on voltage production and anodic ORP.

4.5 Correlation between growth curve and redox potential change in MFC

The growth pattern of *B. subtilis* in anodic chamber and batch condition with LB broth as substrate and the redox potential behaviors of the anodic chamber were reported for the operating condition at pH 8 and aeration rate of 11.32 vvm at 25°C. As seen in Figure 4.4, there were three distinguished growth phases present, including lag phase, exponential phase, and stationary phase. *B. subtilis* required a prolonged period for cell replication, and the lag phase extended to 7 h to

complete compared to the batch fermentation of 3-4 h. The exponential phase was observed from 8 h to 28 h after fermentation started with O.D. of 1.88-1.90. The stationary phase was observed at 30 h, and O.D. of 1.91 was resulted by the end of MFC experiment. The death phase was not observed. By comparing the O.D. between fermentation of *B. subtilis* in MFC and batch conditions, the bacterial growth in an anodic chamber required a prolonged period for cell multiplication. Eventually, the population size and cell mass of MFC fermentation were smaller than that obtained from batch fermentation. *B. subtilis* was an obligate aerobe with ample metabolic repertoire but limited anaerobic growth may occur when an electron acceptor was insufficient or specific electron acceptors were present (Rödel & Lücke, 1990). The reason for inferior bacterial growth MFC fermentation may be that the anodic environment only provided partial oxygen demand and a lack of electron acceptor to complete the metabolic cycle required by bacterial cell development.

Over the entire course of the fermentation run, the redox potential level in the anodic chamber was ranged from -415 to 35 mV. During the lag phase, the *B. subtilis* was adapted to the environmental condition in the medium. Only a slight change of redox potential occurred (±10mV). Most of the variation in redox potential change observed in this period was due to the experimental error. When the growth of *B. subtilis* entered the exponential phase, the redox potential dramatically decreased from 25.3 mV to -370 mV from 7 up to 20 h of fermentation. This change indicated that the metabolic activity and microbial growth significantly increased in the exponential phase. After 20 h of operation, the growth of *B. subtilis* reached the stationary phase. The redox potential then kept descending, but the tendency to decrease turned slowly to the end of the experiment. This observation inferred that the growth and the metabolic activity were slower in the anodic chamber. The minor fluctuation of redox potential was also observed during this phase of growth, possibly due to continuously sparging air and agitation in the anodic chamber, causing the increase of oxygen content and redox potential. Still, oxygen was rapidly consumed by *B. subtilis* for cell growth and metabolism and against the rise of redox potential. Near the end of the fermentation, the lowest redox potential was observed at -418 mV. This redox potential and the cell growth curve corresponded to the finding originally reported by Lin, Chien & Duan (2010). However, the lowest trough and trend of increase of redox potential were not observed in this experiment. This discrepancy could be attributed to the insufficient fermentation time in this experiment, and *B. subtilis* still presented vigorous vitality and substrate not depleted at the end of

the experiment (72 h). The result was consistent with Hongo et al. (1972), who suggested that the ORP was strictly related to cell growth.

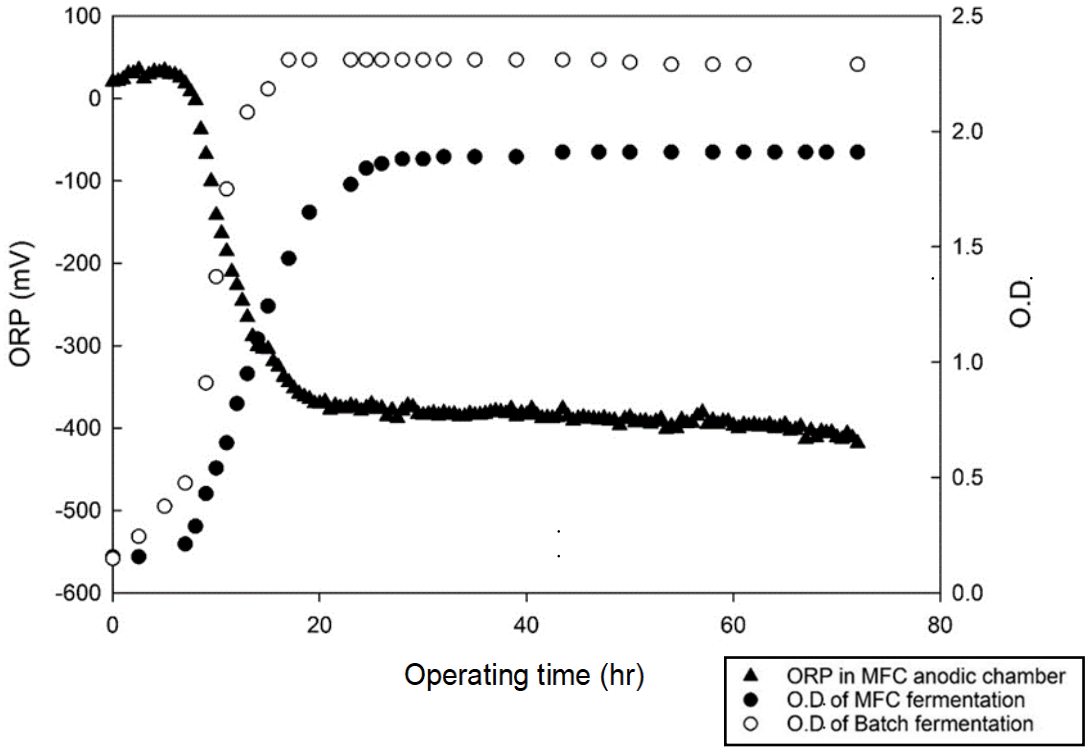

Figure 4.4 Growth of *Bacillus subtilis* under batch and MFC condition and redox potential change of anodic chamber in MFC device vs. time.

4.6 Correlation between growth curve and voltage output from MFC

Figure 4.5 showed the change in voltage vs. cell activity. The voltage increased steadily over 72 h of the experiment. The stable voltage of 6.17 mV was observed at 3.5 h, which was in *B. subtilis*'s lag phase, and the bacteria were adapting to the environment and trying to accumulate more biomass. Afterward, the output of voltage was attributed to the significant growth of biomass; the voltage reached more than 100 mV after 17 h of operation. Interestingly, the rise in voltage stopped and decreased slightly for a short period from 18-20 h, indicating the transition from the exponential growth phase to the stationary phase. From this point, the O.D. value reached 1.89, and the output voltage increased linearly to 336.12 mV at 72 h.

The results revealed a strong correlation between *B. subtilis* growth and voltage output from the MFC. The accumulation of the *B. subtilis* population in the lag phase provided extra energy to the kick-start reactions and overcame the overpotential. The first voltage from the MFC

indicated that the *B. subtilis* population started to grow. At this time, the bacterial cells established a connection with the electrode and began shuttling electrons through the external circuitry to complete their metabolic cycle.

The linear voltage increases of 20 h was due to the continuous growth of the biofilm on the electrode. Logan et al. (2007) and Malvankar et al. (2011) suggested that MFC voltage generation's capacity mainly depended on the electrode surface area and projection area between the electrode and bacterial biofilm.

From 20 to 72 h, the bacterial population was at its maximum – yet the expanding biofilm generates an ever-increasing voltage. Theoretically, the voltage would eventually peak when the maximum biofilm projection area was achieved, or the substrate was depleted. In our experiment, the observed linear rise in voltage was inadequate to elucidate the underlying bacterial growth dynamics.

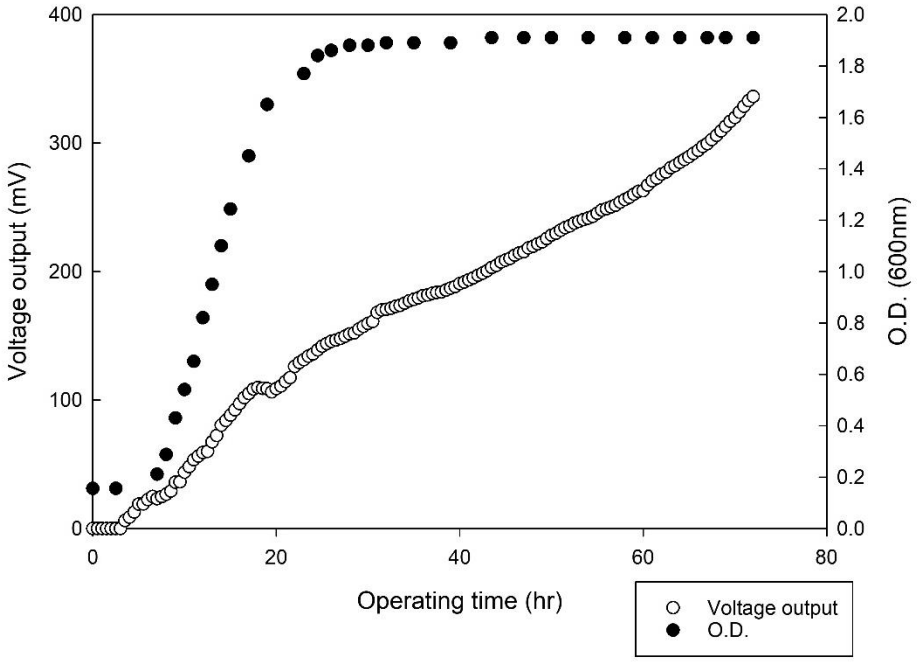

Figure 4.5 The growth of *Bacillus subtilis* and voltage output from MFC system by bacteria cell activity vs. time.

4.7 Correlation analysis from potential parameter ($X = e^{-\frac{\Delta ORP}{\Delta V}}$)

The Nernst Equation evaluated the relation of reduction potential and the standard electrode potential with given conditions. In Section 4.1, the original Nernst equation was reformulated to adapt to the MFC condition, in which a unitless potential parameter X correlates the fermentation redox potential and cell potential (voltage) was derived (Equation 3.5).

Figure 4.6 illustrated the intercorrelation between the potential parameter X and bacterial growth by plotting the potential parament X, ORP, O.D., and d(O.D.)/dt vs. time. As seen in Figure 4.6, there were 2 peaks found along the potential parameter X curve. The potential parameter x was 0 till 6 h of culturing. While *B. subtilis* growth left lag phase and entered the exponential phase, the O.D. and potential parameter X increased dramatically, and the ORP decreased significantly. The rise of potential parameters peaked around 12-13 h after inoculation, and the curve started to decline rapidly afterward. When the potential parameter X curve peaked, the d(O.D.)/dt is also peaked, which revealed the bacterial strain underwent the most rapid stage during growth. The second peak was observed at approximately 19–20 h culturing time. While the second peak reached in potential parameter X, the d(O.D.)/dt proceeded a sharped decrease. The change of O.D. and ORP had been leveled off, indicating the deceleration of bacterial growth and the growth phase transited from the exponential phase into stationary phase. After the second peak, the potential parameter curve rapid declined between 22-24 h and then gradually decreased over time till the end of the experiment.

The results suggested a correlation between the potential parameter and bacterial growth under MFC conditions. The initial increase of the potential parameter curve indicated the microbial strain thriving growth after the lag phase, and the population size increased significantly. While the first peak was reached, the d(O.D.)/dt also reached its maximal value, which revealed that *B. subtilis* underwent the most rapid cell propagation and population enlargement at the midpoint of the exponential phase. As the second peak arrived, the growth of *B. subtilis* started to decline simultaneously. The ORP and the growth curve indicated that the exponential phase was closed to the end. Overall, the potential parameter X presented real-time, highly responsive, and high-resolution information that revealed the start of the exponential phase, the midpoint of the exponential phase, and the onset of the stationary phase. Compared to other microbial growth monitoring parameters (O.D. and ORP), the O.D. can not operate in real-time; the measurement process is time-consuming and labor-intensive. And the O.D. substantially is a turbidimetric

assessment that is prone to error, and the change of O.D. is delayed towards the actual microbial growth dynamics. On the other hand, ORP is a versatile parameter, but it only presents the potential parameter's partial information. The advantage of potential parameter X combined the ORP and voltage measurement, which not only evaluated the external environmental condition change (ΔORP) triggered by microbial growth but also took the internal metabolic activities and actual microbial performance (ΔV) into account. Hence, the potential parameter X provided an insightful understanding of bacterial growth dynamics and enabled precise fermentation monitoring and controlling.

Therefore, based on our findings, the potential parameter derived from Nernst Equation could be applied to the MFC and presented a strict correlation to the cell growth dynamics.

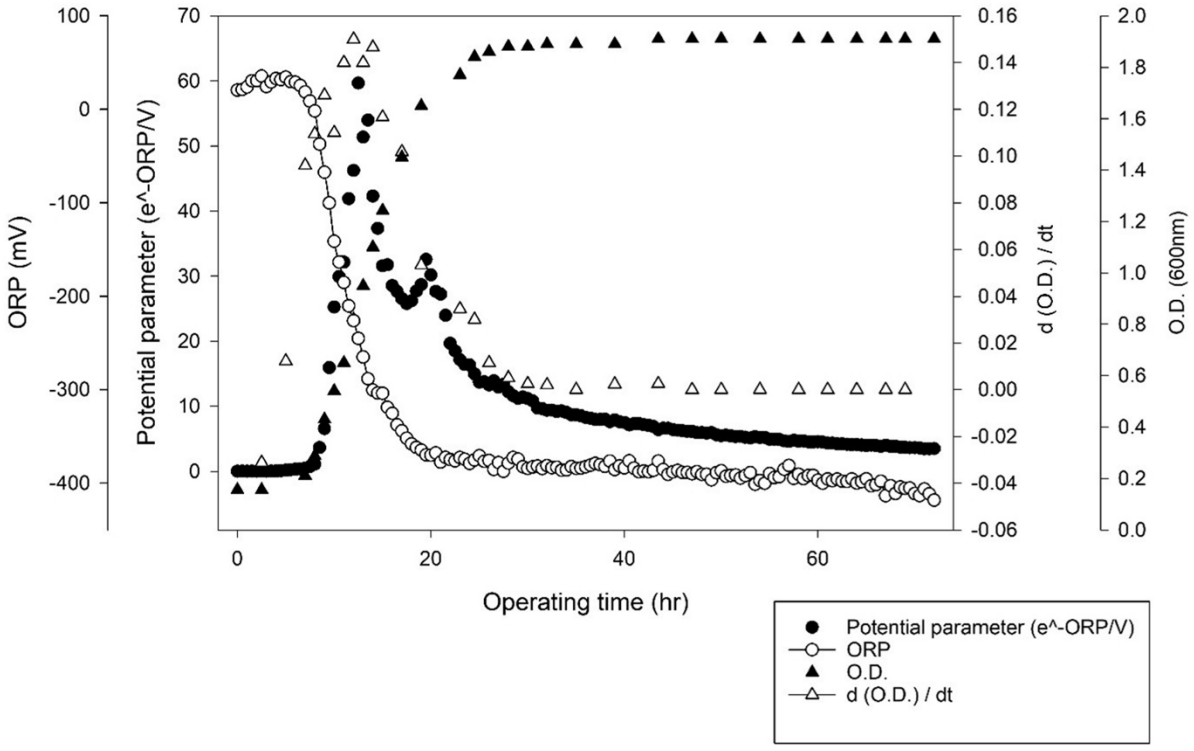

Figure 4.6 Profiles of potential parameter, ORP, optical density, and change of optical density of *B. subtilis* in 72 h.

5 CONCLUSION AND RECOMMENDATIONS

This study set out to provide a step-by-step experimental design to prove the concept of utilizing the MFC as the fermentation ORP sensor. MFC-based fermentation biosensor enabled in-situ, real-time, and precise fermentation monitoring and provided a practical, economically feasible alternative for traditional ORP probes. The modified Nernst equation offers a thoughtful insight into integrating the MFC system's voltage and redox potential. A relationship among voltage production, redox potential change, and bacterial growth dynamics could be correlated. Compared to ORP monitoring, such a relationship elucidates the fermentation kinetics by incorporating external chemical profiles and bacteria's internal metabolic performance.

This study lays the groundwork for future research into the novel biosensor research. Despite these promising results, several interesting questions remained unaddressed. MFCs are sensitive to factors such as temperature and pH – which also played an important role in the Nernst equation (Kyazze et al., 2010). Other environmental conditions may impact the essential correlations delineated in this work. Lastly, this research should employ other bacteria/bacterial-consortia, other growth media, and other MFC architectures.

The first step in this study was to investigate the feasibility of different bacteria. Two common bacteria with distinct physiological characters, *B. subtilis* and *P. fluorescens* were selected as candidates. The *B. subtilis* present better adaptation, rapid growth, and strong power-producing ability in the MFC condition. Different cathode and anode treatments have also been considered and compared in this study. This study had tested other electron acceptors (oxygen, potassium ferricyanide) and different cathode treatments (aerated, sparging), and the result revealed that sparging is a better choice among different treatments by considering the functionality and simplicity. The effect of anode aeration rate of 0, 11.32, 22.64 vvm had been investigated in this study as well. The result suggested that aeration at 11.32 vvm would enhance microbial growth and further support biosensor function. Finally, integrating all the above knowledge gained from the experiments, voltage, ORP, and O.D. from MFC over time had been plotted. The voltage curve presented a flat increase corresponding to the bacterial growth, and it is inadequate to elucidate the

underlying bacterial growth dynamics. Although the ORP curve presented a strict relationship to the O.D. change, only one peak represented the shifting from lag to the exponential phase. By utilizing the potential parameter derived from the modified Nernst equation, a tight relationship was portrayed among the MFC output, fermentation ORP, and bacterial growth dynamics. The potential parameter presented a detailed and high-resolution curve, with higher sensitivity to monitoring the bacterial growth dynamic than ORP and voltage alone. Such a method provides insight for understanding the fermentation bioprocess.

A limitation in this study is that investigation only emphasis the electrochemical performance and the relationship between bacteria and fermentation dynamics. The metabolic flux, multi-omics analysis, and specific electrochemical assay are not researched. Whilst this study only constructs a laboratory-scale simplified MFC under optimal conditions, it did substantiate the concept of an alternative real-time MFC biosensor. Disparate from the traditional BOD/COD MFC-based biosensor, this novel MFC biosensor monitored internal ORP change, and integrated with the voltage generation to achieve the fermentation monitoring function. Possible future work could be done in two different directions:

1. Apply the result and experience gained from this study and develop a versatile, miniature MFC-based biosensor. Such biosensors could apply not only for industrial fermentation but also for soil, wastewater, and oenological research.
2. Investigate the specific physiological adaption of bacteria in the MFC-base biosensor and utilize high-throughput technology to enable metabolomics, transcriptomic, and proteinic research. Construct specific strain that specialized for the MFC-based biosensor.

6 REFERENCES

Allen, J. F. (1993). control of gene expression by redox potential and the requirement for chloroplast and mitochondrial genomes. *Journal of Theoretical Biology, 165*(4), 609-631. doi:10.1006/jtbi.1993.1210

Allen, R. M., & Bennetto, H. P. (1993). Microbial fuel-cells: Electricity production from carbohydrates. *Appl Biochem Biotechnol, 39*(27), 27–40.

Asveld, L., & Van Est, R. (2011). Getting to the core of the bio-economy A perspective on the sustainable promise of biomass. In. Netherlands.

Bonan, C. I. D. G., Biazi, L. E., Dionísio, S. R., Soares, L. B., Tramontina, R., Sousa, A. S., . . . Ienczak, J. L. (2020). Redox potential as a key parameter for monitoring and optimization of xylose fermentation with yeast Spathaspora passalidarum under limited-oxygen conditions. *Bioprocess and Biosystems Engineering, 43*(8), 1509-1519. doi:10.1007/s00449-020-02344-2

Cantó, C., Menzies, J., Keir, & Auwerx, J. (2015). nad+ metabolism and the control of energy homeostasis: a balancing act between mitochondria and the nucleus. *Cell Metabolism, 22*(1), 31-53. doi:10.1016/j.cmet.2015.05.023

Chang, Cheng, H.-B., & Chao, A. C. (2004). applying the nernst equation to simulate redox potential variations for biological nitrification and denitrification processes. *Environmental Science & Technology, 38*(6), 1807-1812. doi:10.1021/es021088e

Chang, S.-H., Wu, C.-H., Wang, R.-C., & Lin, C.-W. (2017). Electricity production and benzene removal from groundwater using low-cost mini tubular microbial fuel cells in a monitoring well. *Journal of Environmental Management, 193*, 551-557.

Chaudhuri, S. K., & Lovely, D. R. (2003). Electricity generation by direct oxidation of glucose in mediatorless microbial fuel cells. *Nat Biotechnol.*, 1229-1232.

Chen, B.-Y., Ma, C.-M., Han, K., Yueh, P.-L., Qin, L.-J., & Hsueh, C.-C. (2016). Influence of textile dye and decolorized metabolites on microbial fuel cell-assisted bioremediation. *Bioresource Technology, 200*, 1033-1038.

Chouler, J., & Di Lorenzo, M. (2015). water quality monitoring in developing countries; can microbial fuel cells be the answer? *Biosensors (Basel), 5*(3), 450-470. doi:10.3390/bios5030450Cohen, B. (1931). The bacterial culture as an electrical half-cell. *Bacteriol, 21*, 18-19.

Cohen, B., Chambers, R., & Reznikoff, P. (1928). intracellular oxidation-reduction studies : i. reduction potentials of amoeba dubia by micro injection of indicators. *J Gen Physiol, 11*(5), 585-612. doi:10.1085/jgp.11.5.585

Coton, M., Pawtowski, A., Taminiau, B., Burgaud, G., Deniel, F., Coulloumme-Labarthe, L., Coton, E. (2017). Unraveling microbial ecology of industrial-scale Kombucha fermentations by metabarcoding and culture-based methods. *FEMS Microbiology Ecology, 93*(5). doi:10.1093/femsec/fix048

Creasey, R., Mostert, B., Nguyen, T., Virdis, B., Freguia, S., & Laycock, B. (2018). Microbial nanowires – Electron transport and the role of synthetic analogues. *Acta Biomaterialia, 69*, 1-30.

Cui, Y., Lai, B., & Tang, X. (2019). Microbial Fuel Cell-Based Biosensors. *Biosensors (Basel), 9*(3). doi:10.3390/bios9030092

Davis, J. B., & Yarbrough, H. F. (1962). preliminary experiments on a microbial fuel cell. *Science, 137*(3530), 615-616.

Delord, B., Neri, W., Bertaux, K., Derre, A., Ly, I., Mano, N., & Poulin, P. (2017). Carbon nanotube fiber mats for microbial fuel cell electrodes. *Bioresour Technol, 243*, 1227-1231. doi:10.1016/j.biortech.2017.06.170

Di Lorenzo, M., Thomson, A. R., Schneider, K., Cameron, P. J., & Ieropoulos, I. (2014). A small-scale air-cathode microbial fuel cell for on-line monitoring of water quality. *Biosensors and Bioelectronics, 62*, 182-188. doi:https://doi.org/10.1016/j.bios.2014.06.050

Do, M. H., Ngo, H. H., Guo, W., Chang, S. W., Nguyen, D. D., Liu, Y., . . . Kumar, M. (2020). Microbial fuel cell-based biosensor for online monitoring wastewater quality: A critical review. *Science of The Total Environment, 712*, 135612. doi:https://doi.org/10.1016/j.scitotenv.2019.135612

Du, Z., Li, H., & Gu, T. (2007). A state of the art review on microbial fuel cells: A promising technology for wastewater treatment and bioenergy. *Biotechnology Advances, 25*, 464-482.

Emde, R., Swain, A., & Schink, B. (1989). Anaerobic oxidation of glycerol by Escherichia coli in an amperometric poised-potential culture system. *Applied Microbiology and Biotechnology, 32*(2), 170-175.

Evelyn, Li, Y., Marshall, A., & Gostomski, P. A. (2014). Gaseous pollutant treatment and electricity generation in microbial fuel cells (MFCs) utilising redox mediators. *Reviews in Environmental Science and Biotechnology*, 35-51.

Feiner, A.-S., & McEvoy, A. (1994). The nernst equation. *Journal of Chemical Education, 71*(6), 493.

Ferguson, J. B. (1923). The oxides of iron. *Journal of the Washington Academy of Sciences, 13*(13), 275-281.

Foyer, C. H., & Noctor, G. (2005). redox homeostasis and antioxidant signaling: a metabolic interface between stress perception and physiological responses. *The Plant Cell, 17*(7), 1866-1875. doi:10.1105/tpc.105.033589

Ghasemi, M., Wan Daud, W. R., Ismail, M., Rahimnejad, M., Ismail, A. F., Leong, J. X., Ben Liew, K. (2013). Effect of pre-treatment and biofouling of proton exchange membrane on microbial fuel cell performance. *International Journal of Hydrogen Energy, 38*(13), 5480-5484. doi:10.1016/j.ijhydene.2012.09.148

Glaser, P., Danchin, A., Kunst, F., Zuber, P., & Nakano, M. M. (1995). Identification and isolation of a gene required for nitrate assimilation and anaerobic growth of Bacillus subtilis. *Journal of Bacteriology, 177*(4), 1112-1115. doi:10.1128/jb.177.4.1112-1115.1995

Gorby, Y. A., Yania, S., McLean, J. S., Rosso, K. M., Moyles, D., Dohnalkova, A., . . . Fredrickson, J. K. (2006). Electrically conductive bacterial nanowires produced by Shewanella oneidensis strain MR-1 and other microorganisms. *Proc Natl Acad Sci U S A, 103*(30), 11358–11363.

GrandViewResearch. (2019). *Fermentation Chemicals Market Size, Share & Trends Analysis Report By Product (Alcohols, Enzymes), By Application (Industrial, Plastic, Pharmaceutical), By Region, And Segment Forecasts, 2019 - 2025*. Retrieved from

He, Z., Minteer, S. D., & Angenent, L. T. (2005). Electricity generation from artificial wastewater using an upflow microbial fuel cell. *Environmental Science and Technology, 39*(14), 5262-5267.

He, Z., Wagner, N., Minteer, S. D., & Angenent, L. T. (2006). An upflow microbial fuel cell with an interior cathode: Assessment of the internal resistance by impedance spectroscopy. *Environmental Science and Technology, 40*(17), 5212-5217.

Hoffmann, T., Troup, B., Szabo, A., Hungerer, C., & Jahn, D. (1995). The anaerobic life of Bacillus subtilis: Cloning of the genes encoding the respiratory nitrate reductase system. *FEMS Microbiology Letters, 131*(2), 219-225. doi:10.1111/j.1574-6968.1995.tb07780.x

Hongo, M., Ishizaki, A., & Uyeda, M. (1972). studies on oxidation-reduction potentials (orp) of microbial cultures. *Agricultural and Biological Chemistry, 36*(1), 141-145. doi:10.1080/00021369.1972.10860221

Huang, X., & Lin, Y. H. (2020). Reconstruction and analysis of a three-compartment genome-scale metabolic model for Pseudomonas fluorescens. *Biotechnology and Applied Biochemistry, 67*(1), 133-139. doi:10.1002/bab.1852

Humphrey, A. E., & Lee, S. E. (1992). Industrial Fermentation: Principles, Processes, and Products. In J. A. Kent (Ed.), *Riegel's Handbook of Industrial Chemistry* (pp. 916-986). Dordrecht: Springer Netherlands.

Ishizaki, A., Shibai, H., & Hirose, Y. (1974). basic aspects of electrode potential change in submerged fermentation. *Agricultural and Biological Chemistry, 38*(12), 2399-2406. doi:10.1080/00021369.1974.10861537

Ismail, Z. Z., & Jaeel, A. J. (2013). Sustainable power generation in continuous flow microbial fuel cell treating actual wastewater: influence of biocatalyst type on electricity production. *The Scientific World Journal, 2013*, 1-7. doi:10.1155/2013/713515

Jensen, W. B. (1996). electronegativity from avogadro to pauling: part 1: origins of the electronegativity concept. *Journal of Chemical Education, 73*(1), 11. doi:10.1021/ed073p11

Jiang, H., Halverson, L. J., & Dong, L. (2015). A miniature microbial fuel cell with conducting nanofibers-based 3D porous biofilm. *Journal of Micromechanics and Microengineering, 25*(12), 1-15.

Jones, D. P., & Sies, H. (2015). The redox code. *Antioxidants & redox signaling, 23*(9), 734-746.

Kakarla, R., Kim, J. R., Jeon, B.-H., & Min, B. (2015). Enhanced performance of an air–cathode microbial fuel cell with oxygen supply from an externally connected algal bioreactor. *Bioresource Technology, 195*, 210-216. doi:10.1016/j.biortech.2015.06.062

Kalathil, S., Patil, S. A., & Pant, D. (2018). microbial fuel cells: electrode materials. In K. Wandelt (Ed.), *Encyclopedia of Interfacial Chemistry* (pp. 309-318). Oxford: Elsevier.

Karamanou, M., & Androutsos, G. (2013). Antoine-Laurent de Lavoisier (1743–1794) and the birth of respiratory physiology. *Thorax, 68*(10), 978-979. doi:10.1136/thoraxjnl-2013-203840

Killeen, D. J., Boulton, R., & Knoesen, A. (2018). advanced monitoring and control of redox potential in wine fermentation. *American Journal of Enology and Viticulture*, ajev.2018.17063. doi:10.5344/ajev.2018.17063

Kim, B. H., Kim, H. J., Hyun, M. S., & Park, D. H. (1999). Direct electrode reaction of Fe(III)-reducing bacterium, Shewanella putrifaciens. *J Microbiol Biotechnol*, 127-131.

Kolodkin-Gal, I., Elsholz, A. K. W., Muth, C., Girguis, P. R., Kolter, R., & Losick, R. (2013). Respiration control of multicellularity in Bacillus subtilis by a complex of the cytochrome chain with a membrane-embedded histidine kinase. *Genes & Development, 27*(8), 887-899. doi:10.1101/gad.215244.113

Kovárová-Kovar, K., & Egli, T. (1998). Growth kinetics of suspended microbial cells: from single-substrate-controlled growth to mixed-substrate kinetics. *Microbiology and molecular biology reviews : MMBR, 62*(3), 646-666. doi:10.1128/MMBR.62.3.646-666.1998

Kyazze, G., Popov, A., Dinsdale, R., Esteves, S., Hawkes, F., Premier, G., & Guwy, A. (2010). Influence of catholyte pH and temperature on hydrogen production from acetate using a two chamber concentric tubular microbial electrolysis cell. *International Journal of Hydrogen Energy, 35*(15), 7716-7722. doi:https://doi.org/10.1016/j.ijhydene.2010.05.036

Lande, A. D. L., Babcock, N. S., Řezáč, J., Lévy, B., Sanders, B. C., & Salahub, D. R. (2012). Quantum effects in biological electron transfer. *Physical Chemistry Chemical Physics, 14*(17), 5902. doi:10.1039/c2cp21823b

Lawson, K., Rossi, R., Regan, J. M., & Logan, B. E. (2020). Impact of cathodic electron acceptor on microbial fuel cell internal resistance. *Bioresource Technology, 316*, 123919. doi:https://doi.org/10.1016/j.biortech.2020.123919

Li, W.-W., Sheng, G.-P., Liu, X.-W., & Yu, H.-Q. (2011). Recent advances in the separators for microbial fuel cells. *Bioresource Technology*, 244-252.

Li, X., Zheng, R., Zhang, X., Liu, Z., Zhu, R., & Zhang, X. (2019). A novel exoelectrogen from microbial fuel cell: Bioremediation of marinepetroleum hydrocarbon pollutants. *Journal of Environmental Management, 235*, 70-76.

Lin, Y.-H., Chien, W.-S., & Duan, K.-J. (2010). Correlations between reduction–oxidation potential profiles and growth patterns of Saccharomyces cerevisiae during very-high-gravity fermentation. Process Biochemistry, 45(5), 765-770. doi:10.1016/j.procbio.2010.01.018

Liu, Xue, C., Lin, Y., & Bai, F. (2013). Redox potential control and applications in microaerobic and anaerobic fermentations. *Biotechnol Adv, 31*(2), 257-265. doi:10.1016/j.biotechadv.2012.11.005

Liu, C., Qin, J.-C., & Lin, Y.-H. (2017). Fermentation and redox potential. *Fermentation Processes. IntechOpen*, 23-42.

Liu, H., & Logan, B. E. (2004). electricity generation using an air-cathode single chamber microbial fuel cell in the presence and absence of a proton exchange membrane. *Environmental Science Technology, 38*, 4040-4046.

Liu, Z., Liu, J., Zhang, S., Xing, X.-H., & Su, Z. (2011). Microbial fuel cell based biosensor for in situ monitoring of anaerobic digestion process. *Bioresource Technology*, *102*(22), 10221-10229. doi:https://doi.org/10.1016/j.biortech.2011.08.053

Logan, B., Cheng, S., Watson, V., & Estadt, G. (2007). graphite fiber brush anodes for increased power production in air-cathode microbial fuel cells. *Environmental Science & Technology*, *41*(9), 3341-3346. doi:10.1021/es062644y

Logan, B., Hamelers, B., Rozendal, R., Schroder, U., Keller, J., Freguia, S., . . . Rabaey, K. (2006). microbial fuel cells: methology and technology. *Environmental Science & Technology*, *40*(17), 5181-5192.

Logan, B. E. (2009). Exoelectrogenic bacteria that power microbial fuel cells. *Nature Reviews Microbiology, 7*, 375-381.

Lohar, S. A., Patil, V. D., & Patil, D. B. (2015). role of mediators in microbial fuel cell for generation of electricity and waste water treatment. *International Journal of Chemical Sciences, 6*, 7-11.

Lovley, D. (2006). Bug juice: harvesting electricity with microorganisms. *Nature Reviews Microbiology, 4*, 497-508.

Lovley, D. R. (2008). The microbe electric: conversion of organic matter to electricity. *Current Opinion in Biotechnology, 19*(6), 564-571. doi:10.1016/j.copbio.2008.10.005

Mahadevan, A., Gunawardena, D. A., & Fernando, S. (2014). biochemical and electrochemical perspectives of the anode of a microbial fuel cell. In *Technology and Application of Microbial Fuel Cells* (pp. 13–32): Intech Open.

Malvankar, N. S., Vargas, M., Nevin, K. P., Franks, A. E., Leang, C., Kim, B.-C., . . . Lovley, D. R. (2011). Tunable metallic-like conductivity in microbial nanowire networks. *Nature Nanotechnology, 6*(9), 573-579. doi:10.1038/nnano.2011.119

Marcus, R. A. (1956). On the theory of oxidation-reduction reactions involving electron transfer. I. *The Journal of Chemical Physics, 24*(5), 966-978. doi:10.1063/1.1742723

Marcus, R. A., & Sutin, N. (1985). Electron transfers in chemistry and biology. *Biochimica et Biophysica Acta (BBA) - Reviews on Bioenergetics, 811*(3), 265-322. doi:10.1016/0304-4173(85)90014-x

María Martínez-Espinosa, R. (2020). Introductory Chapter: A brief overview on fermentation and challenges for the next future. In *New Advances on Fermentation Processes*: IntechOpen.

Mckenney, P. T., Driks, A., & Eichenberger, P. (2013). The Bacillus subtilis endospore: assembly and functions of the multilayered coat. *Nature Reviews Microbiology, 11*(1), 33-44. doi:10.1038/nrmicro2921

Mohan, S. V., Raghavulu, S. V., Srikanth, S., & Sarma, P. N. (2007). Bioelectricity production by mediatorless microbial fuel cell under acidophilic condition using wastewater as substrate: Influence of substrate loading rate. *Current Science, 92*(12), 1720-1726. Retrieved from http://www.jstor.org/stable/24107621

Morris, J. M., & Jin, S. (2008). Feasibility of using microbial fuel cell technology for bioremediation of hydrocarbons in groundwater. *Journal of Environmental Science and Health, Part A*, 18–23.

Mulchandani, A. (1998). Principles of enzyme biosensors. In A. Mulchandani & K. R. Rogers (Eds.), *Enzyme and Microbial Biosensors: Techniques and Protocols* (pp. 3-14). Totowa, NJ: Humana Press.

Nakano, M. M., Dailly, Y. P., Zuber, P., & Clark, D. P. (1997). Characterization of anaerobic fermentative growth of Bacillus subtilis: identification of fermentation end products and genes required for growth. *Journal of Bacteriology, 179*(21), 6749-6755. doi:10.1128/jb.179.21.6749-6755.1997

Nakano, M. M., & Zuber, P. (1998). Anaerobic growth of a "strict aerobe" (Bacillus subtilis). *Annual Review of Microbiology, 52*(1), 165-190. doi:10.1146/annurev.micro.52.1.165

Needham, J., & Needham, D. M. (1926). The oxidation-reduction potential of protoplasm: A review. *Protoplasma, 1*(1), 255-294. doi:10.1007/bf01602996

Nimje, V. R., Chen, C.-Y., Chen, C.-C., Jean, J.-S., Reddy, A. S., Fan, C.-W., . . . Chen, J.-L. (2009). Stable and high energy generation by a strain of Bacillus subtilis in a microbial fuel cell. *Journal of Power Sources, 190*(2), 258-263. doi:10.1016/j.jpowsour.2009.01.019

Oh, S.-E., & Logan, B. E. (2006). Proton exchange membrane and electrode surface areas as factors that affect power generation in microbial fuel cells. *Applied Microbiology and Biotechnology, 70*(2), 162-169. doi:10.1007/s00253-005-0066-y

Oliveira, V. B., Simoes, M., Melo, L. F., & Pinto, A. M. F. R. (2013). Overview on the developments of microbial fuel cells. *Biochemical Engineering Journal, 73*, 53-64.

Park, S. H., Kim, E. H., Chang, H. J., Yoon, S. Z., Yoon, J. W., Cho, S.-J., & Ryu, Y.-H. (2013). history of bioelectrical study and the electrophysiology of the primo vascular system. *Evidence-Based Complementary and Alternative Medicine*.

Paul, A., Laurila, T., Vuorinen, V., & Divinski, S. V. (2014). Fick's laws of diffusion. In *Thermodynamics, Diffusion and the Kirkendall Effect in Solids* (pp. 115-139): Springer International Publishing.

Peixoto, L., Min, B., Martins, G., Brito, A. G., Kroff, P., Parpot, P., . . . Nogueira, R. (2011). In situ microbial fuel cell-based biosensor for organic carbon. *Bioelectrochemistry, 81*(2), 99-103. doi:https://doi.org/10.1016/j.bioelechem.2011.02.002

Pepè Sciarria, T., Arioli, S., Gargari, G., Mora, D., & Adani, F. (2019). Monitoring microbial communities' dynamics during the start-up of microbial fuel cells by high-throughput screening techniques. *Biotechnology Reports, 21*, e00310. doi:https://doi.org/10.1016/j.btre.2019.e00310

Potter, M. C. (1912). electrical effects accompanying the decomposition of organic compound. *Proceedings of the Royal Society of London, 84*(260).

Pous, N., Puig, S., Coma, M., & Balaguer, M. D. (2013). feasibility of using bioelectrochemical systems for bioremediation. *Bioremediation of nitrate-pollutedgroundwater in a microbial fuel cell*, *88*, 1690–1696.

Rabaey, K., Boon, N., Siciliano, S., Verhaege, M., & Verstraete, W. (2004). biofuel cells select for microbial consortia that self-mediate electron transfer. *Applied and Environmental Microbiology, 70*(9), 5373-5382.

Rahimnejad, M., Adhami, A., Darvari, S., Zirepour, A., & Oh, S. E. (2015). Microbial fuel cell as new technol ogy for bioelectricity generation: A review. *Alexandria Engineering Journal, 54*(3), 745-756.

Reguera, G., McCarthy, K. D., Mehta, T., Nicoll, J. S., Tuominen, M. T., & Lovley, D. R. (2005). Extracellular electron transfer via microbial nanowires. *Nature, 435*(7045), 1098-1101.

Ringeisen, B. R., Henderson, E., Wu, P. K., Pietron, J., Ray, R., Little, B., . . . Jones-Meehan, J. M. (2006). High power density from a miniature microbial fuel cell using Shewanella oneidensis DSP10. *Environmental Science and Technology, 40*(8), 2629-2634.

Rismani-Yazdi, H., Carver, S. M., Christy, A. D., & Tuovinen, O. H. (2008). Cathodic limitations in microbial fuel cells: An overview. *Journal of Power Sources, 180*(2), 683-694. doi:10.1016/j.jpowsour.2008.02.074

Rödel, W., & Lücke, F.-K. (1990). Effect of redox potential on Bacillus subtilis and Bacillus licheniformis in broth and in pasteurized sausage mixtures. *International Journal of Food Microbiology, 10*(3-4), 291-301. doi:10.1016/0168-1605(90)90076-h

Rohrback, G. H., Scott, W. R., & Canfield, J. H. (1962). Biochemical fuel cells. *Power sources conference., 16*, 18-21.

Sangeetha, T., & Muthukumar, M. (2012). influence of electrode material and electrode distance on bioelectricity production from sago-processing wastewater using microbial fuel cell. *Environmental Progress & Sustainable Energy, 32*(2), 390-395.

Schafer, F. Q., & Buettner, G. R. (2001). Redox environment of the cell as viewed through the redox state of the glutathione disulfide/glutathione couple. *Free Radical Biology and Medicine, 30*(11), 1191-1212. doi:10.1016/s0891-5849(01)00480-4

Scholz, F. (2017). Wilhelm Ostwald's role in the genesis and evolution of the Nernst equation. *Journal of Solid State Electrochemistry, 21*(7), 1847-1859. doi:10.1007/s10008-017-3619-y

Schroder, U. (2007). Anodic electron transfer mechanisms in microbial fuel cells and their energy efficiency. *Physical Chemistry Chemical Physics, 9*(21), 2619-2629. Retrieved from https://pubs.rsc.org/en/content/articlepdf/2007/cp/b703627m

Shapiro, H. M. (1972). Redox balance in the body: An approach to quantitation. *Journal of Surgical Research, 13*(3), 138-152. doi:10.1016/0022-4804(72)90057-1

Shi, L., Squier, T. C., Zachara, J. M., & Fredrickson, J. K. (2007). Respiration of metal (hydr)oxides by Shewanella and Geobacter: A key role for multihaem c-type cytochromes. *Molecular Microbiology, 65*(1), 12-20.

Singh, A., & Yakhmi, J. (2014). Microbial fuel cells – Applications for generation of electrical power and beyond. *Critical Reviews in Microbiology*, 1-17.

Song, H.-L., Zhu, Y., & Li, J. (in press). Electron transfer mechanisms, characteristicsand applications of biological cathode microbialfuel cells – A mini review. *Arabian Journal of Chemistry*.

Su, L., Jia, W., Hou, C., & Lei, Y. (2011). Microbial biosensors: A review. *Biosensors and Bioelectronics, 26*(5), 1788-1799. doi:https://doi.org/10.1016/j.bios.2010.09.005

Suslow, T. V. (2004). Oxidation-reduction potential (orp) for water disinfection monitoring, control, and documentation. doi:10.3733/ucanr.8149

Torres, C. I., Marcus, A. K., Lee, H. S., Parameswaran, P., Krajmalnik-Brown, R., & Rittmann, B. E. (2010). A kinetic perspective on extracellular electron transfer by anode-respiring bacteria. *FEMS Microbiology Reviews, 34*(1), 3-17.

Ucar, D., Zhang, Y., & Angelidaki, I. (2017). An overview of electron acceptors in microbial fuel cells. *Frontiers in Microbiology, 8*(643). doi:10.3389/fmicb.2017.00643

Uria, N., Ferrera, I., & Mas, J. (2017). Electrochemical performance and microbial community profiles in microbial fuel cells in relation to electron transfer mechanisms. *BMC Microbiology, 17*(1), 1-12.

Vargas, M., Malvankar, N. S., Tremblay, P.-L., Leang, C., Smith, J. A., Patel, P., . . . Lovley, D. R. (2013). aromatic amino acids required for pili conductivity and long- range extracellular electron transport in geobacter sulfurreducens. *microbiology, 106*(23), e00105-00113.

Vejarano, F., Benítez-Campo, N., Bravo, E., Loaiza, O. A., & Lizcano-Valbuena, W. H. (2018). Electrochemical Monitoring and Microbial Characterization of a Domestic Wastewater-

Fed Microbial Fuel Cell Inoculated with Anaerobic Sludge. *Revista de Ciencias, 22*, 13-32. doi:https://doi.org/10.25100/rc.v22i2.7910

Vellingiri, A., Song, Y. E., Munussami, G., Kim, C., Park, C., Jeon, B. H., . . . Kim, J. R. (2019). Overexpression of c-type cytochrome, CymA in Shewanella oneidensis MR-1 for enhanced bioelectricity generation and cell growth in a microbial fuel cell. *Journal of Chemical Technology and Biotechnology, 94*(7), 2115-2122.

Wang, R.-S., Oldham, W. M., Maron, B. A., & Loscalzo, J. (2018). systems biology approaches to redox metabolism in stress and disease states. *Antioxidants & redox signaling, 29*(10), 953-972. doi:10.1089/ars.2017.7256

Weibel, M. K., & Dodge, C. (1975). Biochemical fuel cells. Demonstration of an obligatory pathway involving an external circuit for the enzymatically catalyzed aerobic oxidation of glucose. *Arch Biochem Biophys., 169*(1), 146-151.

Yaropolov, A. I., Varfolomeev, S. D., & Berezin, I. V. (1976). Bioelectrocatalysis. activation of a cathode oxygen reduction in the peroxidase-mediator carbon electrode system. *Febs Letter, 71*(2), 306-308.

Yong, Y.-C., Yu, Y.-Y., Li, C.-M., Zhong, J.-J., & Song, H. (2011). Bioelectricity enhancement via overexpression of quorum sensing system in Pseudomonas aeruginosa-inoculated microbial fuel cells. *Biosensors and Bioelectronics, 30*(1), 87-92. doi:https://doi.org/10.1016/j.bios.2011.08.032

Zhang, X. C., & Halme, A. (1995). Modelling of a microbial fuel cell process. *Biotechnology Letters, 17*(8), 809-814. doi:10.1007/BF00129009

Zhao, L., Brouwer, J., Naviaux, J., & Hochbaum, A. (2014, 2014-06-30). *Modeling of Polarization Losses of a Microbial Fuel Cell.* Paper presented at the ASME 2014 12th International Conference on Fuel Cell Science, Engineering and Technology.

Zhou, S., Huang, S., Li, Y., Zhao, N., Li, H., Angelidaki, I., & Zhang, Y. (2018). Microbial fuel cell-based biosensor for toxic carbon monoxide monitoring. *Talanta, 186*, 368-371. doi:https://doi.org/10.1016/j.talanta.2018.04.084

Zhu, J.-G., Ji, X.-J., Huang, H., Du, J., Li, S., & Ding, Y.-Y. (2009). Production of 3-hydroxypropionic acid by recombinant Klebsiella pneumoniae based on aeration and ORP controlled strategy. *Korean Journal of Chemical Engineering, 26*(6), 1679-1685.

Zilberman, D., & Kim, E. (2011). The lessons of fermentation for the new bio-economy. *Agbioforum (Columbia, Mo.), 14*(3), 97-103.

7 APPENDICES

7.1 Appendix A MFC apparatus and instrumentation

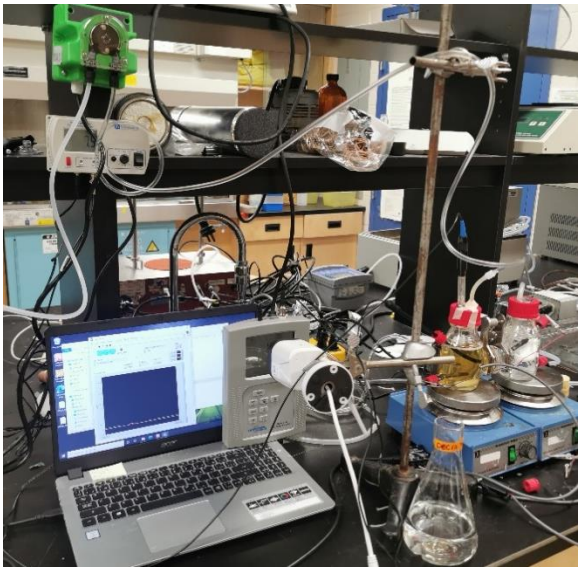

Figure 7.1 Actual MFC-based biosensor laboratory setup

Figure 7.2 Spectrophotometer for bacterial growth monitoring

7.2 Appendix B pH profile during fermentation

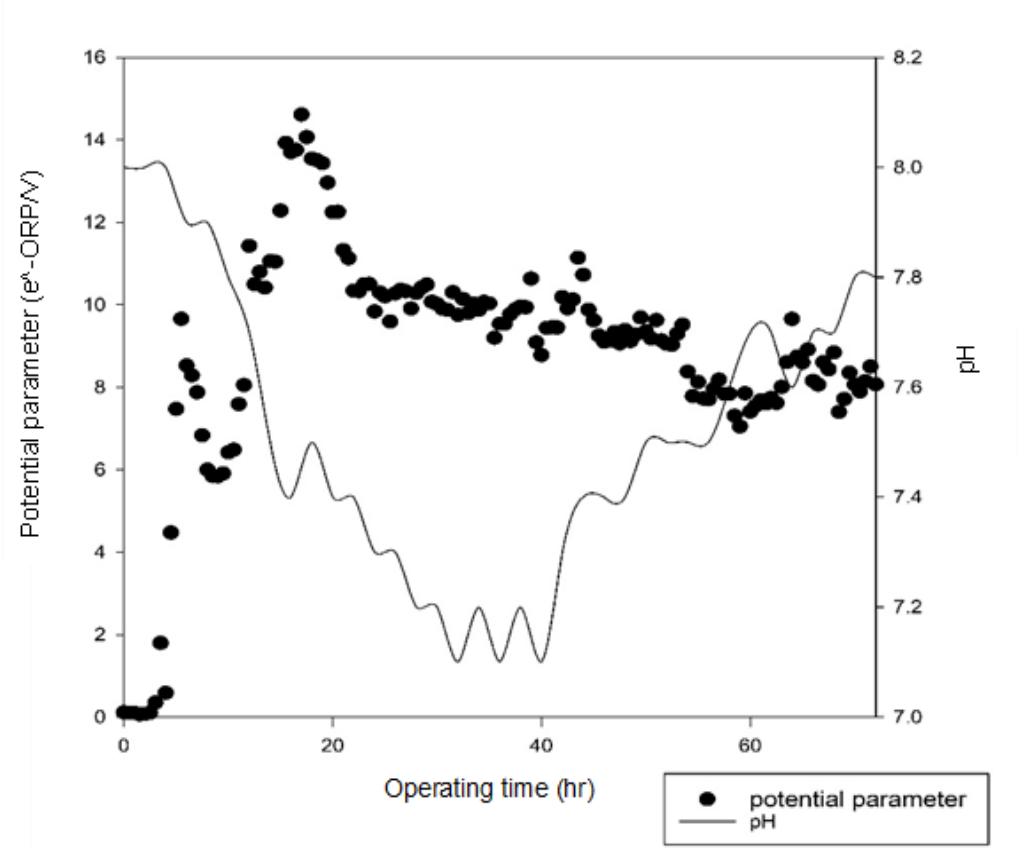

Figure 7.3 pH profile during the MFC fermentation, the potential parameter presents random dispersion of change without introduces pH regulator